NBSIR ~~85-3383~~

Report Number 13

Examination of Failed Railroad Car Wheel/Axle Assembly From Derailed Passenger Car, McIntosh, Georgia

T.R. Shives, S.R. Low, III, and C.H. Brady

U.S. DEPARTMENT OF COMMERCE
National Bureau of Standards
Institute for Materials Science and Engineering
Fracture and Deformation Division
Gaithersburg, MD 20899

August 1985

Failure Analysis Report

Issued June 1986

Prepared for
Federal Railroad Administration
Washington, DC 20590

NBSIR 85-3383

Report Number

EXAMINATION OF FAILED RAILROAD CAR WHEEL/AXLE ASSEMBLY FROM DERAILED PASSENGER CAR, McINTOSH, GEORGIA

T.R. Shives, S.R. Low, III, and C.H. Brady

U.S. DEPARTMENT OF COMMERCE
National Bureau of Standards
Institute for Materials Science and Engineering
Fracture and Deformation Division
Gaithersburg, MD 20899

August 1985

Failure Analysis Report

Issued June 1986

Prepared for
Federal Railroad Administration
Washington, DC 20590

U.S. DEPARTMENT OF COMMERCE, Malcolm Baldrige, *Secretary*
NATIONAL BUREAU OF STANDARDS, Ernest Ambler, *Director*

TABLE OF CONTENTS

TABLE OF CONTENTS

Summary

At the Request of the Federal Railroad Administration, the National Bureau of Standards conducted an examination of a failed wheel assembly from an Amtrak passenger car involved in a derailment at McIntosh, Georgia. The west lead wheel of the trailing truck of the car was found to have a radial fracture which permitted the wheel to move laterally along the axle. The east wheel had suffered a chordal fracture. The apparent sequence of events is the radial fracture of the west wheel followed by lateral motion of that wheel along the axle which permitted the east wheel to drop in the gauge of the track causing the derailment. The fracture of the east wheel was thought to be a result of the derailment.

The west wheel fractured from a crack that initiated at the outside of the tread. There was evidence of a pre-existing crack in the fracture path near the fracture origin, although it is not clear that this crack initiated the fracture. The fracture of the east wheel also intiated at the outside of the tread. There was a gouge near the fracture origin and the fracture passed through a dent, but it is not clear that there is any relationship between either of these areas of mechanical damage and the fracture.

In addition to the fracture crack, two radial cracks were found at the tread of the west wheel. One of these cracks was associated with an inclusion.

Although both wheels appear basically to satisfy AAR specifications for B-36 wheels, some dimensions did not comply and hardness of the west wheel was marginal in some places.

Examination of Failed Railroad Car Wheel/Axle Assembly from Derailed Passenger Car, McIntosh, Georgia

1. INTRODUCTION

1.1. Reference

The work reported herein was performed by the National Bureau of Standards (NBS) at the request of the Federal Railroad Administration (FRA) and was carried out at the direction of Mr. David Dancer and Ms. Claire Orth of the FRA.

1.2. Background

The information in this section was furnished by the Federal Railroad Administration (FRA). An Amtrak passenger train consisting of two locomotives and 15 cars was traveling at 79 mph southbound on the Seaboard Coast Line Railroad single main track at McIntosh, Georgia, when the third through the 15th car derailed. An examination of the derailed equipment revealed that the west lead wheel on the trailing truck of the third car (Amtrak 2766 - Savannah) had a crack extending from the tread to the axle. The east wheel on the same axle was also found to be fractured. Markings on the wheels were reported to be as follows:

West Wheel: F-68345 B 0375 GRADE B-36
East Wheel: F-68341 B 0375 GRADE B-36

According to the FRA, a preliminary examination indicated that the fractured west wheel became loose on the axle permitting the east wheel to drop in the gauge of the track. It was thought that the east wheel eventually fractured as a consequence of the derailment.

1.3 Parts Submitted

The wheel/axle assembly parts submitted for examination are shown as-received at NBS in figures 1 and 2. The assembly consisted of the two wheels, the axle, two axle bearings, and a gear box mechanism at the center of the axle. The east wheel, designated wheel F1 in this report, is at the right in figure 1. The hub of this wheel was still in its correct position on the axle when submitted to NBS. Wheel F1 had suffered a chordal, through-thickness fracture, as shown in figure 1 and again at higher magnification in figure 3. The mating piece of wheel F1 is shown in figure 2. The two mating parts of this wheel were designated F1L and F1S according to their relative size (L for larger and S for smaller).

The west wheel, designated wheel F2 in this report, is at the left in figure 1. This wheel was laterally displaced inboard along the axle and had suffered a through-thickness radial fracture from the hub to the tread (figure 4).

1.4 Work Requested by the FRA

Work requested by the FRA included the following:

a. A list of all identifying marks on the wheels and axle.
b. Detailed illustrations of physical features such as flat spots, external signs of heat, tread and flange condition, micrometer readings of the wheel bores and the axle wheel seat diameters, manufacturing defects, etc.
c. Analysis of the fractures.

d. Macro and micro etching of wheel cross sections, especially in tread and flange areas.
e. Physical, chemical and metallurgical analyses of wheel materials including hardness and carbon content. Results should be compared with AAR specifications.
f. Wheels and axle inspection for cracks and internal flaws.

2. PURPOSE

The purpose of this examination was two-fold:

1) To determine the most probable cause of failure of the wheels and wheel/axle assembly.
2) To determine conformance of the wheels and wheel material to AAR specifications.

3. PREPARATION OF SPECIMENS FOR EXAMINATION AND TESTING

3.1 Dismantling the Wheel/Axle Assembly

In order to facilitate examination and testing of the wheels and axle, it was necessary to remove the wheels from the axle with as little damage as possible to any of the components. The assembly was very carefully dismantled in accordance with instructions from NBS Fracture and Deformation Division personnel at the Fruit Growers Express, a local railroad car manufacturing shop. While at the car shop, wheel F2 was torch cut along a radius approximately 150° from the radial fracture in order to expose the fracture surfaces. The two mating pieces from this wheel, designated F2L and F2S according to their relative size, are shown in figure 5. The axle is shown in figure 6 after the wheels, bearings and gear box had been removed.

3.2 Sectioning of the Wheel Pieces

After the wheel/axle assembly had been dismantled and wheel F2 had been torch-cut, each of the four wheel parts (F1L, F1S, F2L, and F2S) were sectioned by band sawing in the NBS shops to facilitate fracture and materials analysis. Wheel piece F1S was sectioned in accordance with the schematic drawing shown in figure 7. Initially, two pie-shaped pieces, each containing part of the fracture surface adjacent to the wheel tread, were removed. These smaller pieces were designated F1SB1 and F1SA1. An additional 3/4 inch thick section adjacent to each of the pie-shaped pieces was removed from wheel piece F1S. These additional pieces were designated F1SB2 and F1SA2 as shown in figure 7.

Four sections were removed from wheel piece F1L, which is shown in figure 8. Section F1LB1, which contained the entire fracture surface of wheel piece F1L, was separated by a straight saw cut that intersected the edge of the wheel hub and that was essentially equidistant from the fracture at both places where the fracture intersected the wheel tread. Two 3/4 inch thick sections and one 3-3/4 inch thick section between the wheel hub and tread and parallel to the initial section F1LB1 were removed. These smaller pieces were designated F1LB2, F1LB3, and F1LB4, respectively, with increasing distance from the fracture surface.

A 3/4 inch thick section containing the entire fracture surface was removed from wheel pieces F2L and F2S as indicated in the schematic drawing in figure 9. These sections were separated by saw cutting parallel to the fracture and were designated F2SB1 and F2LA1. An additional 3/4 inch thick section adjacent to each of the pieces containing the fracture was also removed. These pieces were designated F2SB2 and F2LA2. A three inch thick section containing the torch-cut surface was removed from piece F2S. This section was designated F2SC1.

Further sectioning of these smaller pieces from either wheel was carried out in the Fracture and Deformation Division Laboratory.

Wheel piece F1SA2 had a section designated I removed adjacent to the tread (figure 10), although not until hardness measurements had been made on the surface. Four sections were removed from wheel piece F1SB2 as shown in figure 11. Sections D, B, and K were used for chemical composition analysis.

A number of sections were removed from wheel piece F2LA2 as shown in figure 12. Sections H2, I2, L and M were used for chemical composition analysis. Sections A, C, D, and E were used for metallographic examination of the wheel material microstructure. Sections A, B, C, D and M were used for inclusion measurements.

Two sections, designated A1 and A2, were removed from wheel piece F2SB1 as shown in figure 13. Each of these sections was then cut parallel to the fracture in order to remove the fracture surface. The parts containing the fracture maintained the designations A1 and A2, whereas the pieces from which the fracture was cut were designated A1B and A2B, respectively. These specimens were used for Knoop microindentation hardness measurements. The part of wheel piece F2SB1 below the horizontal white line in figure 13 was sent to Mr. David Dancer of the FRA in August, 1979.

A section for chemical composition analysis was taken from the web of wheel piece F2SB2 as shown in figure 14.

4. RESULTS OF EXAMINATIONS AND TESTS

4.1 Visual Examination

A careful examination of both wheels was made to determine the presence of identifying markings such as those indicated by the FRA in Section 1.1 of this report. Whereas, it had been reported that wheel F1 (east wheel) had been marked "F-68341 B 0375 Grade B-36," no such marking, or for that matter, no marking of any kind was found on this wheel.

On wheel F2 (west wheel), the following characters were found in barely visible yellow paint: "75 68345." The reported designation for this wheel was "F-68345 B 0375 Grade B-36".

An examination of the axle revealed stamped markings at each end. At the east end (adjacent to the former location of wheel F1), the following markings were found: MF6 1749 SSW 6 26 49 55 MF2 52 MF 10 20 50 FIN Z A9M 6 17 49 SSW 6 23 49. The west end of the axle (adjacent to the former location of wheel F2) was marked: AMT 10609 SSW 76 6 49 CW8358 Z A9M.

Both pieces F1L and F1S from wheel F1 had suffered considerable mechanical damage to the tread. There were numerous gouges, regions of galling and regions of abrasion on both pieces. The most severly abraded region of the tread of piece F1L is shown in figure 15. Examples of regions of the tread of wheel piece F1L exhibiting galling and gouging are shown in figures 16 and 17, respectively.

An overall view of wheel piece F1S showing damage to the tread appears in figure 18. Gouging and galling of this wheel piece can be seen in figure 19. There was also a flat spot on the tread of this wheel segment (figure 20). The flange of wheel F1 exhibited some mechanical damage, but much less than the tread. The severest flange damage observed was adjacent to the flat spot on the tread.

Wheel F2 exhibited much less mechanical damage than did wheel F1. There were some chips from the tread (figure 21), but none of the deep gouges or severely abraded regions that were evident in wheel F1. There was one region on the flange of wheel piece F2S that exhibited significant mechanical damage (figure 22).

Most of the mechanical damage observed on both wheels is thought to have occurred after, and as a result of, the fracture of wheel F2.

4.2 Fractographic Examination

4.2.1 Visual and Macroscopic Examination

One of the fracture surfaces from wheel F1 (piece F1LB1) is shown in figure 23. The fracture markings clearly indicate that the fracture initiated in the vicinity of the outside corner of the tread (arrow A, figure 23). The mechanical damage suffered by the wheel at this point appears to have occurred after the fracture had taken place. There was, however, a relatively sharp gouge on the outside face about 1/8 inch from the tread that may have been present before the fracture occurred. This gouge, which was about 3/32 inch deep, would have acted as a stress concentrator. Because of the condition of the tread in this region, it can not be said with certainty that the fracture originated at this gouge, but the fracture markings indicate that the origin is either at or very near it.

The fracture passed through a depression or dent (arrow B, figure 23) at the inside of the flange. Parts of this dent were visible in mating locations in both wheel pieces F1L and F1S indicating that it had likely been present before the wheel had fractured. It is not clear whether this dent influenced the fracture. Part of the fracture from wheel piece F1SA1 is shown in figure 24 at higher magnification than figure 23. This fracture surface is the mate to the fracture surface shown in figure 23. The dent on the inside of the flange is indicated by the arrow (figure 24). The mechanical damage evident on the outside of the tread near the apparent fracture origin on piece F1LB1 was not observed on wheel piece F1SA1.

No other mechanical damage was evident that was thought to have contributed to the fracture of this wheel.

One of the fracture surfaces from wheel F2 (piece F2SB1) was previously shown in figure 13. The markings on this fracture surface indicate that the probable initiation site was at the outside edge of the tread (intersection of the tread and the outside face of the wheel). The location of the probable initiation site is indicated by arrow A in figure 13. This region is shown at higher magnification in figure 25. Some of the metal at this location appeared to be "smeared". Optical metallography later revealed that the smeared region consisted of plastically deformed or cold worked material.

Slightly inward along the tread at the location of specimen A2 (arrow B, figure 13), the fracture was covered with a rather tenacious oxide that appeared to be heavier than the oxide on the rest of the fracture surface. This oxide remained on the surface after cleaning for fifteen minutes in an ultrasonic bath, whereas the oxide on the rest of the fracture surface was readily removed. The presence of the heavy oxide suggests that a crack may have existed for a period of time before final fracture occurred. Even so, the fracture markings do not indicate this possible pre-existing crack as the probable fracture initiation site.

4.2.2. Scanning Electron Microscope Examination

Samples A1 and A2 from wheel piece F2SB1 from the fracture of wheel F2 were examined with the scanning electron microscope (SEM). An SEM fractograph showing a field typical of the "smeared" region of the fracture appears in figure 26. Considerable cracking, much of it along apparent grain boundaries, is evident. Many of the fracture features have been obliterated by the cold working (mechanical damage), but there are a few pockets of apparent dimpled rupture indicating at least some ducitility in this part of the fracture. An SEM fractograph typical of the region adjacent to the mechanically damaged region is shown in figure 27. Cleavage is the primary fracture mode exhibited indicating very little ductility in this part of the fracture.

An area adjacent to the tread in the heavily oxidized region is shown in figure 28 after the specimen had been ultrasonically cleaned a second time. The fracture appearance suggests significant corrosion in this area. Slightly further from the tread surface and further in from the outer face of the wheel, the fracture mode was primarily cleavage (figure 29). The area shown in figure 29 is away from the heavily oxidized region. In an area well removed from the tread, but still within specimen A2, the fracture exhibited both dimpled rupture and cleavage (figure 30).

4.3 Dimensional Measurements

Dimensional measurements were made at the locations shown in Table 1 for each wheel to determine conformance to Association of American Railroads (AAR) specifications for B-36 wheels (adopted 1946, revised 1947). Axial measurements were made on piece F1LB3 for wheel F1 and on piece F2SC1 for wheel F2. Radial measurements were made on the unsectioned parts of one or both of the major wheel components. Dimensions were measured with either a calibrated rule or outside locking calipers. Measurements were accurate to within ± 1/32 inch as required by the AAR specification. Results of these measurements, as well as the AAR specification requirements, are given in Table 1. All the dimensions given in Table 1 for both wheels except for A, B, D, and G satisfy the AAR requirements. The larger value for A and the smaller values for D and G could have been caused by

normal wear. Therefore, these dimensions may have satisfied the AAR requirements when the wheels were new. The high values for B, however, would not likely have been caused by wear. Dimension B appears not to satisfy the AAR requirements.

The inside diameter of the wheel hub (bore) was measured on wheel piece F1L. Seven measurements at one inch intervals starting at the front face of the hub were made. The values were very consistent and averaged 7.98 inches. Individual measurements are given in Table 2. The AAR specification calls for a maximum of 8-1/2 inches for the bore; therefore wheel F1 satisfies the specification.

The diameter of the axle was measured where each of the two wheels had been seated. Five measurements were made at the wheel F1 seat and four measurements were made at the wheel F2 seat. The results are given in Table 3.

4.4 Hardness Measurements

4.4.1 Macroindentation Hardness Measurements

Brinell hardness measurements were made on the surfaces of the wheel pieces that were adjacent to the samples containing the fracture surfaces. These surfaces were essentially parallel to the fracture and removed from it by about 3/4 inch. The saw-cut surfaces of the wheel pieces were ground and polished to prepare surfaces suitable for Brinell hardness measurements. Hardness measurement locations were spaced at one-half or three-quarter inch intervals along hub to rim axes.

Measurements were made on three different pieces from wheel F1. Two were rim pieces, F1SA2 and F1SB2, which were located at opposite ends of the fracture. The third piece, F1LB2, ran from the hub to the rim. Measurements for wheel F2 were made on only one piece, F2SB2, which ran from the hub to the rim. The results of the Brinell hardness measurements are shown in figures 31 to 34. In these figures, the hardness values are shown at the locations from which they derived. For comparison, the AAR specification for Class B wheels requires that the hardness be between 277 HB and 341 HB on the front face of the rim not less than 3/16 inch from the radius joining the face and the tread, and that the hardness not exceed 293 HB at any point not more than one-half inch from the bore.

With two exceptions, the measured Brinell hardness values from locations up to 1-1/4 inches from the rim in samples from both wheels satisfied the AAR specification. One exception was a value of 272 HB (5 HB numbers below the required minimum) determined at a location 1/2 inch below the rim in wheel piece F1SA2. The second exception was a value of 275 (3 HB numbers below the required minimum) determined at a location 1-1/2 inches below the rim in wheel piece F1LB2. Brinell hardness measurements taken near the hub in both wheels all satisfied the AAR specification.

Although two of the measured values fell slightly below the minimum requirement of the specification, the locations were away from the rim and neither is considered a serious breach of the specification.

4.4.2. Microindentation Hardness Measurements

Knoop microindentation hardness measurements at a load of 200 gf were made on samples A1B and A2B from wheel piece F2SB1. These two samples were cut from pieces A1 and A2, respectively, which are shown in figure 13. The sample surfaces on which the microindentation hardness measurements were made were polished metallographically prior to testing. The results of the hardness measurements are given in Table 4 and are listed in the order of increasing distance from the tread surface of the wheel. The samples had been etched with picral prior to testing. The comments adjacent to the hardness values in Table 4 reflect the appearance of the microstructure in the etched condition at the location of the hardness measurements. Those locations described as being white, brown or tan exhibit the effects of heat. Locations described as "base metal" do not show the effects of heat. Except for one value about 0.0005 inch from the tread surface in sample A2B1, the hardness of the heat affected areas was significantly greater than that of the material that was unaffected by heat. In fact, the hardness of the heat affected material was very high. The hardness of the material unaffected by heat as measured by the microindentation hardness technique was somewhat higher than the Brinell hardness values on wheel piece F2SB2, but all of the microindentation hardness measurements were taken closer to the tread surface than any of the Brinell measurements.

4.5 Axle Inspection

The entire axle was inspected visually for defects at the surface. In addition, the areas where the wheels and bearings had been seated were examined ultrasonically. A 5 MHz/0.5 inch ceramic transducer was used to look for defects throughout the cross section of the axle. A 5 MHz/0.5 inch dual element transducer was used to look for near-surface defects. The only indication of defects was near the left end (as the axle was oriented in service) where the wheel seated. The apparent defects ran continuously from the end of the spline to the fillet. It is suspected that the "defects" were forging laps that tapered in from the surface to a depth of about 0.5 inch. The "defects" could be seen only from the opposite side and only with the single element transducer.

4.6 Chemical Analyses

Samples from both wheels F1 and F2 were analyzed for chemical composition by an independent testing laboratory. For wheel F1, three samples, designated B, D, and K as shown in figure 11, from wheel piece F1SB2 were analyzed. Samples from two pieces from wheel F2 were analyzed. These included four samples, designated H2, I2, L, and M, from wheel piece F2LA2 and one sample designated D from wheel piece F2SB2. These two wheel pieces were from opposite ends of the fracture in wheel F2. The locations of the samples from these two pieces are shown in figure 12 for piece F2LA2 and in figure 14 for piece F2SB2.

Results of the analyses are given in Table 5. Except where noted, all values shown in Table 5 were determined by spectrographic techniques.

The AAR specification requirements for chemical composition are also given in Table 5 for comparison. It should be noted that there are no AAR specifications for some of the elements for which analyses were made. All spectrographically determined values satisfied the applicable AAR requirement. X-ray fluorescence determinations for sulfur in sample B from wheel

piece F2SB2 and in sample L from wheel piece F2LA2 did not satisfy the specification. Additional analyses by combustion/titration techniques, which are generally superior to x-ray fluorescence methods, resulted in values for sulfur content in both samples that did satisfy the AAR requirements. In fact, values obtained by averaging the results from both the x-ray fluorescence and combustion/titration techniques fall within the accepted range.

4.7 Metallurgical Examination

4.7.1 Inclusion Determination

4.7.1.1 Sulfur Printing

Sulfur prints were made from four wheel pieces, two from each wheel. One sample from each of the large and small pieces of each wheel were used. The sulfur prints were prepared by soaking photographic paper with a silver bromide emulsion in a two percent solution of sulfuric acid, and then pressing the drained, but still wet, paper against the polished surface of the sample for three minutes. After being removed from the sample, the print is fixed, washed and dried in the same way as for a photographic print. A sulfur print is essentially a map of the sulfide inclusions in the steel in the plane where the print is made. The distribution of these inclusions may indicate possible deleterious sulfide segregation. Large sulfide segregations can act like flaws.

No evidence of any significant sulfide inclusion segregation was revealed in the sulfur prints. The inclusions were rather uniformly distributed throughout the samples indicating good homogeneity. Sulfur prints from each of the four samples are shown in figures 35 through 38.

4.7.1.2 Inclusion Density and Size Determination

One region from each wheel was examined for inclusion content. The inclusion content is important to determine because very large inclusions or inclusion concentrations can act as flaws. Two samples, designated F1SB2-D and F1SB2-I, were selected from wheel F1. The locations of these samples can be seen in figure 11. Five samples, designated A, B, C, D, and M were selected from wheel F2 piece F2LA2. The locations of these samples are shown in figure 12. Two methods were used to determine the average inclusion content in each sample. In the first method, an image analyzing computer was used. This device automatically scanned the polished surfaces of the samples optically distinguishing between the light and dark areas. It then computed the percentage dark area in the sample surfaces. Assuming that all the dark areas consisted of inclusions, the percentage inclusions was then equivalent to the percentage dark area. The results as determined by this method are given in Table 6. The inclusion content varied from about 0.23 percent to 0.34 percent.

The second method for determining the inclusion content was in accordance with ASTM Standard E45, Plate I. One field considered to be representative of the material from each of the seven samples was evaluated by the ASTM method. The results are presented in Table 7. There were no significant differences among different samples from either wheel nor between samples from both wheels. Examples of one of the fields used for inclusion determination from each wheel are shown in figures 39 and 40.

4.7.2 Microstructural Examination

4.7.2.1 Macroscopic Examination

Polished samples from both wheels were deep etched with boiling hydrochloric acid for visual and macroscopic examination. Samples F1SB2 and F1LB3 from wheel F1 (figures 7 and 8, respectively) and sample F2SB2 from wheel F2 (figure 14) were deep etched. The material appeared to be homogenous with no evidence of segregation. There was however, a crack in wheel piece F1LB3 parallel and adjacent to the tread. This crack can be seen in figure 41 where part of wheel piece F1LB3 is shown.

4.7.2.2 Metallographic Examination

The metallographic examination was concentrated on wheel F2. There was an area adjacent to the tread of this wheel that had been affected by heat presumably caused by contact between the wheel tread and the rail. The location of this heat affected zone (HAZ) on wheel piece F2LA2 is indicated by the arrow in figure 42. The heat affected zone at another location of the tread (wheel piece F2SB1) is shown at higher magnification in figure 43. (The diamond shaped areas shown in this figure are microindentation hardness impressions.) The heat affected zone consisted principally of untempered martensite. A representative field from the heat affected zone from specimen A, wheel piece F2LA2 is shown in figure 44. The microstructure of the transition zone between the heat affected zone and the unaffected base metal is shown in figure 45. Fine carbides and ferrite are the principal constituents. Well removed from the transition zone and the edge of the sample, the microstructure consisted primarily of pearlite with small patches of ferrite (figure 46).

A zone in specimen E (figure 42) at the wheel hub adjacent to the axle exhibited the effects of heat. A field from specimen E showing this heat affected zone appears in figure 47. The white layer at the surface represents this zone. There are numerous radial cracks in the heat affected zone. Most of the cracks pass all way through the heat affected zone and, as shown in figure 48, some pass into the material which was not affected by heat. The microstructure of the heat affected zone appears to consist primarily of tempered martensite. The zone was apparently produced by relative motion between wheel F2 and the axle. The microstructure adjacent to the HAZ was similar to that shown in figure 46 which was near the tread.

The metallographic examination revealed at least two cracks at the tread surface of wheel F2 that do not appear to be associated with the heat affected zone. The cracks were basically perpendicular to the tread surface. One crack appeared to be associated with inclusions as shown in figure 49, whereas the other does not appear to be associated with inclusions, at least in the plane examined (figure 50).

A small amount of decarburization was evident along the surface of the wheel web on both the inboard and outboard sides. A representative field from the inboard side is shown in figure 51.

5. DISCUSSION

A thorough examination of wheel F1 (east wheel) revealed no identifying marks, although it had been reported that this wheel had had such marks. There were some barely visible painted marks found on wheel F2 (west wheel), but these marks were only part of the identification reported for this wheel. Therefore, neither wheel had the identifying marks that had been reported for it. Both wheels were reported to be of the B-36 type. The axle did have identifying marks.

The approximate location of the fracture initiation site was rather clearly indicated on the fracture surface of each wheel. In both cases, fracture initiated at the outside of the tread. For wheel F2, which appears to have failed first, the fracture crack propagated from the tread to the hub forming a radial fracture. Once this fracture had formed, wheel F2 could move laterally on the axle. The heat affected zone at the hub of this wheel is evidence that the wheel did indeed move on the axle, although not necessarily laterally. However, the wheel apparently did move on the axle in an inward direction which permitted wheel F1 to drop into the gauge of the track resulting in the chordal fracture of this wheel.

Both wheels had suffered a great deal of mechanical damage, but at least most of this damage appears to have occurred as a result of the accident and therefore did not contribute to the failure. The cold work exhibited in the region of the fracture initiation site of wheel F2 appears to have occurred as a result of the accident. A rather tenacious oxide on part of the fracture surface near the initiation site suggests the existence of a crack prior to the time of final fracture. Although close, this apparent preexisting crack is not at the indicated initiation site.

There was a gouge very near the fracture initiation site for wheel F1 that was likely present before the fracture occurred. The fracture also passed through a dent that apparently was present before the fracture. It is not clear, however, that either the gouge or the dent influenced the fracture.

Four of the measured dimensions for each wheel failed to satisfy the AAR requirements for B-36 wheels. The location and amount by which three of these dimensions failed to satisfy the specification could have been caused by normal wear during service and it appears quite likely that these dimensional requirements were met when the wheels were new. The fourth dimension that did not satisfy the AAR specification apparently did not satisfy the specification when the wheels were new. There were no other significant dimensional or property deficiencies observed for either wheel.

Except for two values for wheel F1, Brinell hardness measurement results indicated that, at least away from the surface, the hardness of the wheel material for both wheels satisfied the AAR requirements for B-36 wheels. The two excepted values failed to satisfy the specification by a very small amount. Knoop microindentation hardness measurements taken in and near the heat affected zone adjacent to the tread of wheel F2 indicated the hardness of this zone to be quite high. Metallographic examination of this area revealed untempered martensite as the principal constituent of the microstructure. Untempered martensite is expected to be very hard and

has essentially no ductility. Its presence is very undesirable. However, the heat affected zone, and hence the untempered martensite, probably occurred as a result of the failure rather than having contributed to it. This zone would have resulted from friction between the wheel tread and the rail.

Two radial cracks were found at the tread of wheel F2 in a region not associated with overheating. One of these cracks passed through a subsurface inclusion whereas the other did not. It is not clear what effect cracks such as these might have had on the failure of a wheel.

There was another heat affected zone in wheel F2 in the hub area adjacent to the axle bore. The microstructure here consisted primarily of tempered martensite. Many radial cracks passed throught the heat affected zone, some passing into the unaffected material. This zone was very likely created by friction between the wheel and the axle after the wheel had become loose on the axle. Again, this heat affected zone was a result of the failure of wheel F2 rather than a contributor to it.

The microstructure in regions away from the heat affected zone consisted primarily of pearlite with some ferrite and was considered to be satisfactory. The small amount of decarburization adjacent to both the inboard and outboard surfaces of the web is not considered to be significant. The sulfur prints indicated that, at least for those areas examined, the distribution of sulfur inclusions was relatively uniform with essentially no segregation evident. Inclusion measurements indicated that the inclusion content was not excessive in wheel F2. No determinations were made for wheel F1.

Apparently, the critical issue in the failure of this wheel assembly was the radial fracture in wheel F2 (west wheel). The fracture of the east wheel, as well as most of the mechanical damage to both wheels, appears to have occurred after the fracture of the west wheel and is likely a result of the fracture of the west wheel.

6. CONCLUSIONS

1. Neither wheel from this assembly was marked in accordance with reported FRA information.
2. The west wheel (wheel F2) fractured radially from a crack that initiated at the outside of the tread and propagated to the hub.
3. The cause of crack initiation in the west wheel is not clear, although there was evidence of a pre-existing crack in the fracture path through the west wheel in an area close to the crack initiation site.
4. The fracture of the west wheel appears to have preceded that of the east wheel, (wheel F1) and initiated the failure of the entire wheel assembly.
5. The east wheel fractured along a chord due to a crack that initiated at the outside of the tread and propagated across the wheel.
6. There was a gouge near the fracture origin of the east wheel and the fracture passed through a dent. Both the gouge and the dent were likely present before the fracture occurred, but it is not clear that there is any relationship between either of these areas of mechanical damage and the fracture.

7. Most of the considerable mechanical damage suffered by the wheels apparently occurred after the fracture of the west wheel and was not a factor contributing to the failure.
8. Four of the measured dimensions of each wheel failed to satisfy the Association of American Railroads (AAR) specifications for B-36 wheels. Three of the dimensions could have been out of specification due to normal wear during service. The fourth dimension, however, apparently did not meet specifications when the wheels were new.
9. There were two radial cracks found at the tread of the west wheel; one crack was associated with an inclusion.
10. The microstructure of the wheel material appeared to be satisfactory in all regions examined except for two heat affected zones at the hub and tread that apparently formed at the time of the assembly failure.
11. Except for the heat affected areas, and two other minor exceptions, the hardness of the wheel material satisfied the AAR specification for B-36 wheels.
12. Inclusion distribution was uniform and the size and concentration of the inclusions did not appear to be excesive.
13. The chemical composition of both wheel materials satisfied the AAR requirements, although the analysis indicated that the sulfur content in both was borderline on the high side.

Although these wheels appear basically to satisfy the requirements set forth by the AAR for B-36 wheels, it should be pointed out that some dimensions for both wheels failed to comply, hardness of the west wheel material was marginal in a couple of instances, and the sulfur content was higher than acceptable for both wheels as determined by one analytical technique.

7. Acknowledgement

Dr. Charles G. Interrante of the NBS Metallurgy Division set up the examination plan and most of the work was carried out under his direction.

Table 1. Dimensional Measurements

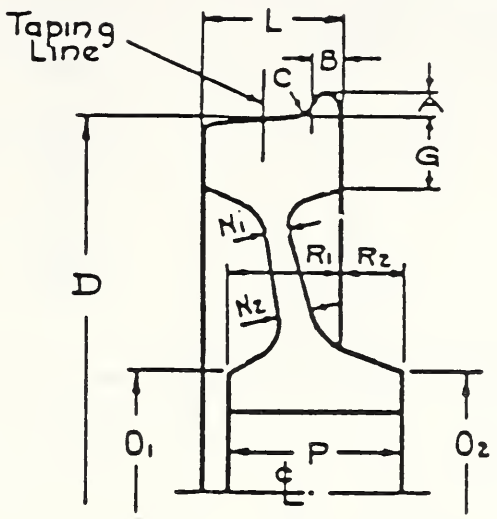

Dimension	AAR Specification	Wheel F1	Wheel F2
A	$1^{+1/16}_{-0}$	1-11/32*	1-10/32***
B	$1\frac{5}{32}^{+1/16}_{-0}$	1-9/32	1-8/32
C	$\frac{11}{16}\pm\frac{1}{16}$	NA	NA
D	$\frac{36}{-0}$ Inches	34-17/32**	NA
G	$2\frac{3}{4}$ Min	2-5/16*	2-7/16***
L	$5\frac{1}{2}\pm\frac{1}{8}$	5-1/2	5-17/32
N1	$\frac{3}{4}$ Min.	13/16	7/8
N2	1 Min	1-1/2	1-1/2
O1	$10\frac{3}{4}^{+1}_{-0}$	11-9/32**	NA
O2	$10\frac{3}{4}^{+1}_{-0}$	11-5/32**	NA
P	$7\pm\frac{1}{8}$	6-15/16	6-29/32
R1	$4\frac{5}{16}^{+0}_{-\frac{1}{8}}$	4-5/16	4-9/32
R2	$2\frac{11}{16}\pm\frac{1}{8}$	2-21/32	2-11/16
Max Finish Bore	$8\frac{1}{2}$	7-31/32	NA
Min Hub Wall	$1\frac{1}{8}$	1-1/2	1-1/2***

All values reported in inches. All dimensions for wheel F1 except for those noted below were measured on wheel piece F1LB3. *Piece F1S, **Piece P1L. All dimensions for wheel F2 except for those noted below were measured on wheel piece F2SC1. ***Piece F2S.

Table 2. Inside Hub Diameter Measurements for Wheel F1.

Distance from front face at bore, inches	Inside hub diameter inches
At front face	7.984
1	7.983
2	7.986
3	7.987
4	7.978
5	7.989
At back face	7.989

Table 3. Axle Diameter Measurements

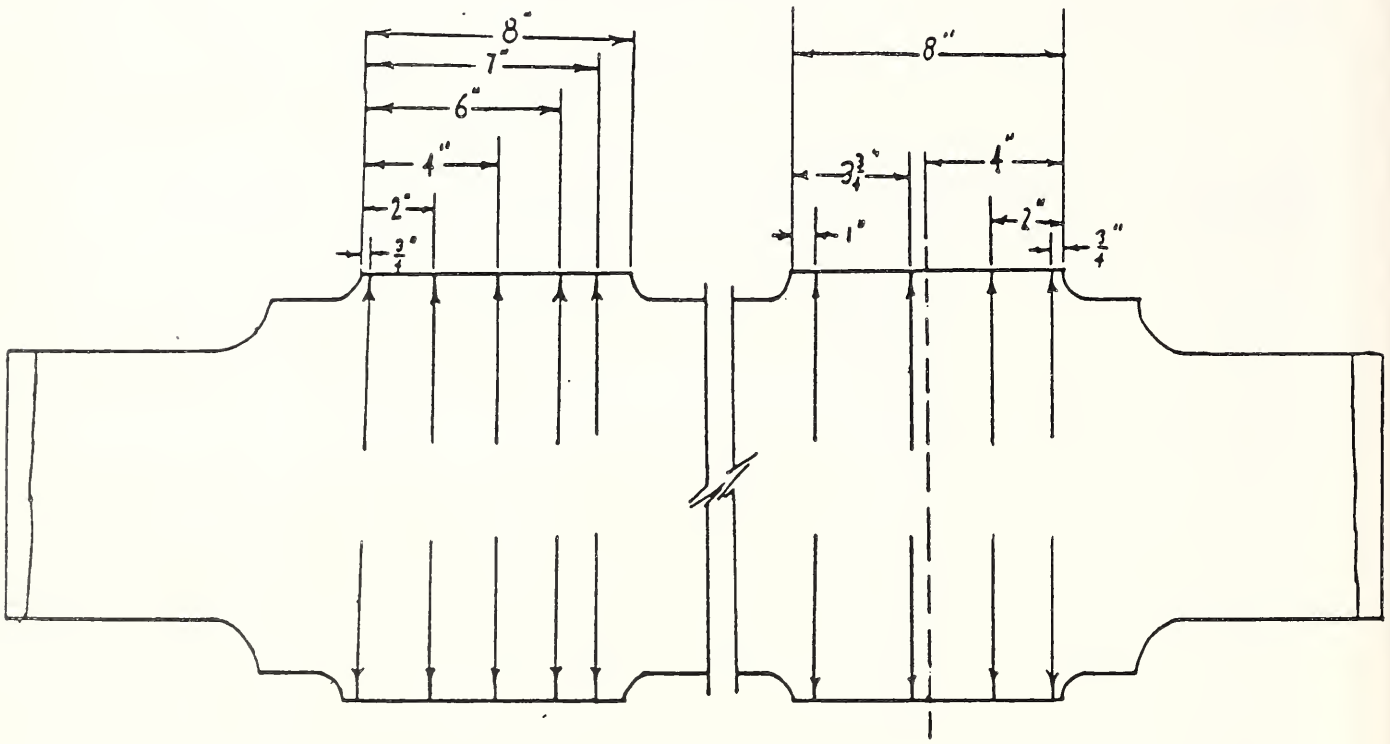

Distance from outside edge of wheel seat, inches	Diameter of axle, inches Wheel F1 (left above)	Wheel F2 (right above)
3/4	7.995	8.001
2	7.995	8.003
4	7.995	
4-3/4		8.003
6	7.996	
7	7.997	8.004

Table 4. Results of Knoop Microindentation Hardness Measurements

Distance from edge of tread, inches	Knoop hardness values, HK 200 Specimen A2B1	A2B2	A2B3
0.0005	434 (white)		776 (tan)
.001	606 (brown)	510 (brown)	
.0015			840 (tan)
.002	812 (tan)	762 (tan)	
.0025			834 (tan)
.003	818 (tan)	812 (tan)	840 (tan)
.004	412 (edge of tan)	807 (tan)	362 (base metal)
.005		698 (tan)	362 (base metal)
.006	383 (base metal)	351 (base metal)	
.007	420 (base metal)		
.008	436 (base metal)	358 (base metal)	
.009	412 (base metal)		
.010	387 (base metal)	366 (base metal)	357 (base metal)
.015	397 (base metal)	405 (base metal)	360 (base metal)
.020		414 (base metal)	
.250			365 (base metal)

Table 5. Results of Chemical Analyses

Element	AAR Spec.	F1SB2-B	F1SB2-D	F1SB2-K	F2LA2-H2	F2LA2-I2	F2LA2-L	F2LA2-M	F2SB2-D
Carbon	0.57-0.67	0.65	0.65	0.64	0.63	0.64	0.62	0.63	0.63
Manganese	0.60-0.85	0.80	0.75	0.79	0.76	0.77	0.76	0.77	0.73
Phosphorus	0.05 max	0.023	0.23	0.023	0.022	0.025	0.022	0.023	0.020
Sulfur*	0.05 max	0.044		0.042	0.038	0.042	0.036	0.046	
Sulfur**	0.05 max	0.055	0.039	0.048	0.041	0.040	0.051	0.048	0.039
Silicon	0.15 min	0.28	0.31	0.28	0.29	0.31	0.30	0.31	0.31
Nickel		0.12	0.15	0.13	0.13	0.14	0.12	0.14	0.13
Chromium		0.19	0.20	0.20	0.20	0.21	0.20	0.21	0.19
Molybdenum		0.05	0.05	0.05	0.05	0.06	0.05	0.06	0.04
Copper		0.35	0.37	0.36	0.36	0.38	0.35	0.36	0.35
Aluminum			0.017						0.018
Vanadium			<0.005						<0.005
Oxygen				0.0060			0.0061		

*Combustion-Titration method
**X-Ray Fluorescence method

Table 6. Results of Percentage Inclusions Measurements

Specimen	Average Percentage Inclusions for 500 Fields
F1SB2-D	0.321
F1SB2-I	0.284
F2LA2-A	0.226
F2LA2-B	0.248
F2LA2-C	0.291
F2LA2-D	0.339
F2LA2-M	0.234

Table 7. Results of Inclusion Rating in Accordance with ASTM Standard E45, Plate I

Specimen	Type Inclusion	ASTM Number	Series
F1SB2-D	A	2-3	thin
F1SB2-I	A	3	heavy
F2LA2-A	A	2-3	heavy
F2LA2-B	A	2	heavy
F2LA2-C	A	2-3	heavy
F2LA2-D	A	2-3	thin
F2LA2-M	A	2-3	heavy

Figure 1. Wheel assembly as received at NBS. The east wheel (F1) is at the right and the west wheel (F2) is at the left.

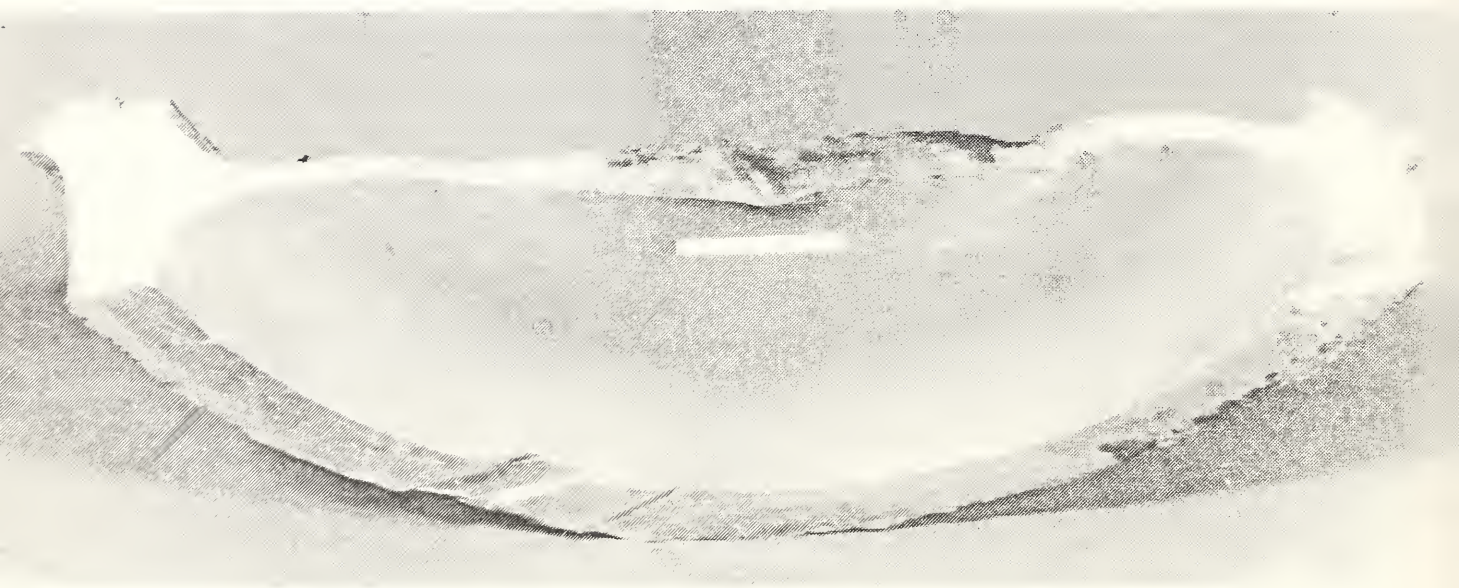

Figure 2. Part of the east wheel (F1) that had fractured from the main part of the wheel. This part is the mate to the part of the wheel shown on the right in figure 1.

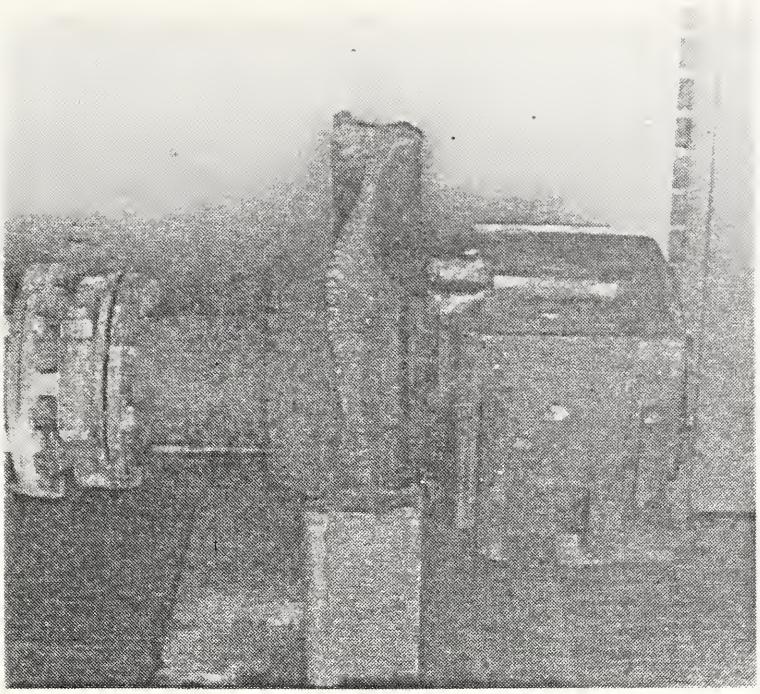

Figure 3. Wheel F1 as received at NBS showing the chordal fracture.

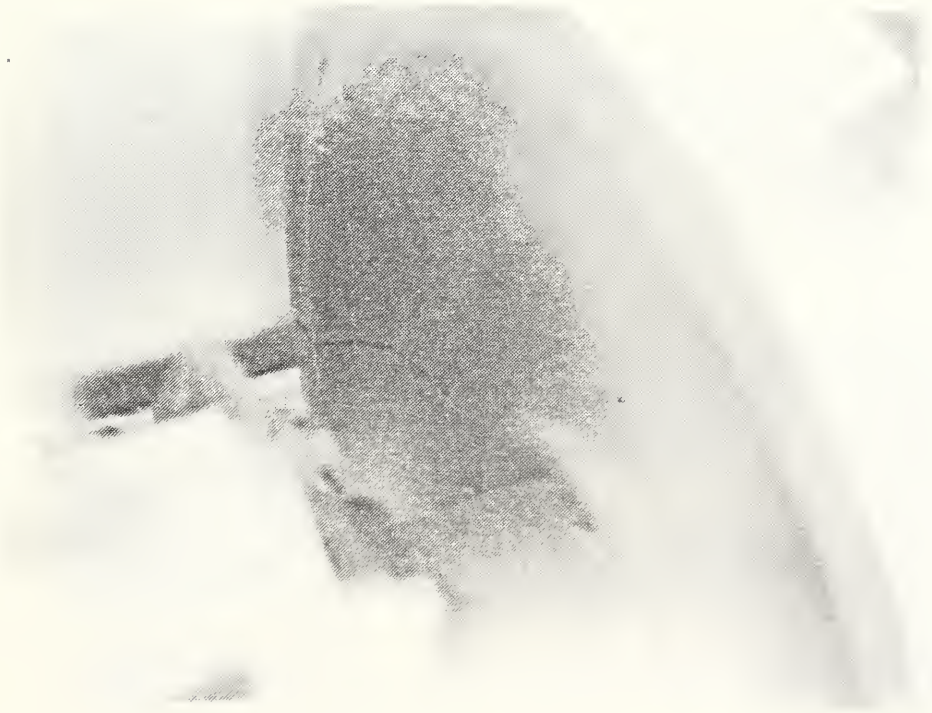

Figure 4. Wheel F2 as received at NBS showing the radial fracture.

Figure 5. The two pieces of wheel F2 after torch cutting. Piece F2L is at the left and piece F2S is at the right.

Figure 6. Axle after the wheel assembly had been dismantled.

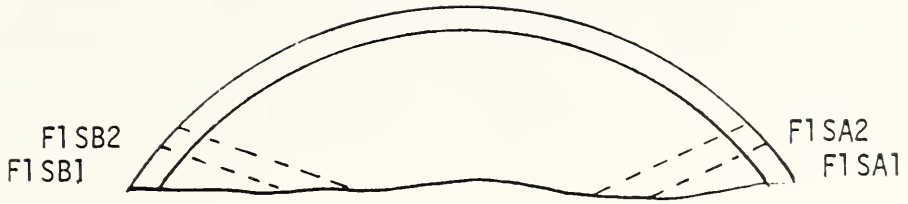

Figure 7. Schematic drawing of wheel piece F1S as viewed from the outside showing where sections were removed by the NBS Shops Division.

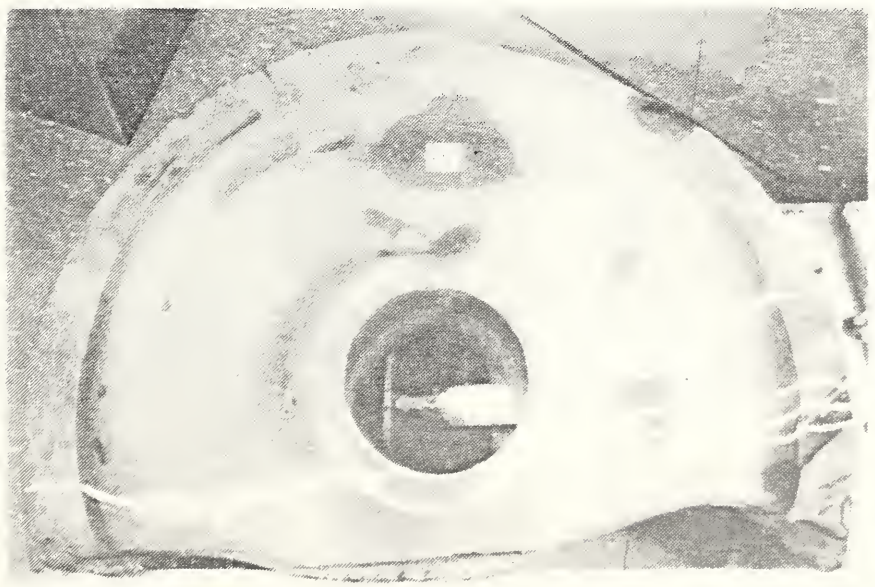

Figure 8. Photograph of wheel piece F1L as viewed from the inside face showing where sections were removed by the NBS Shops Division.

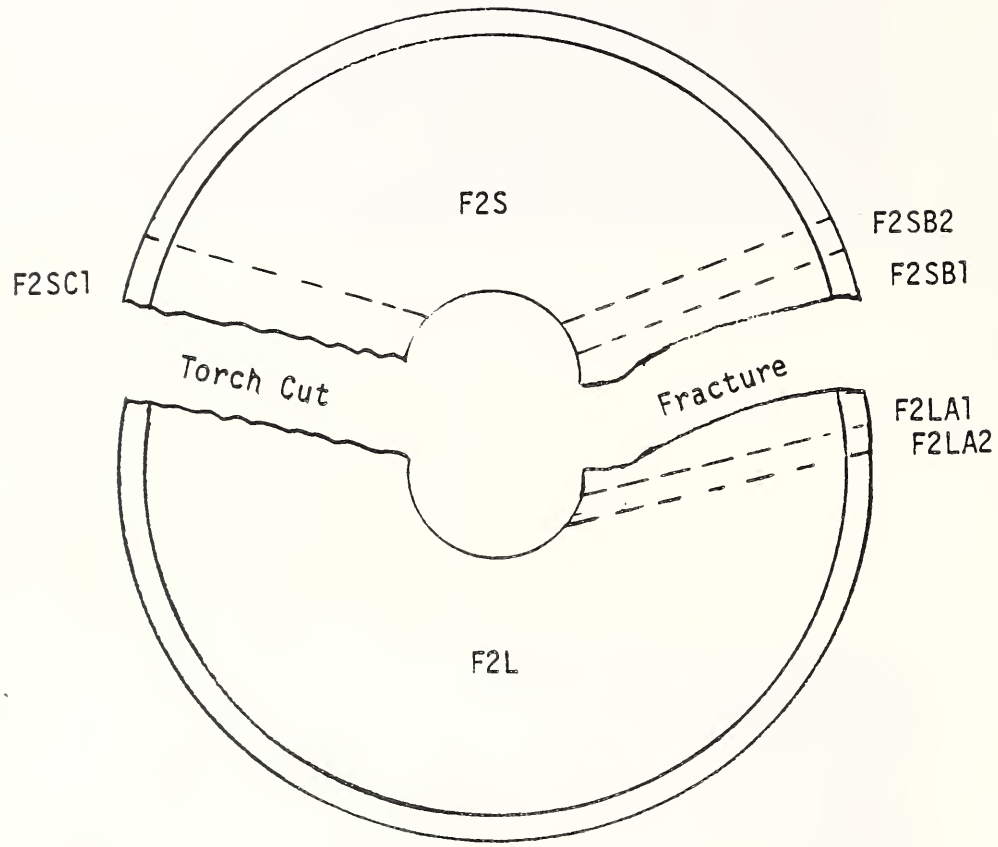

Figure 9. Schematic drawing of wheel F2 as seen from the inside showing the sections removed by the NBS Shops Division.

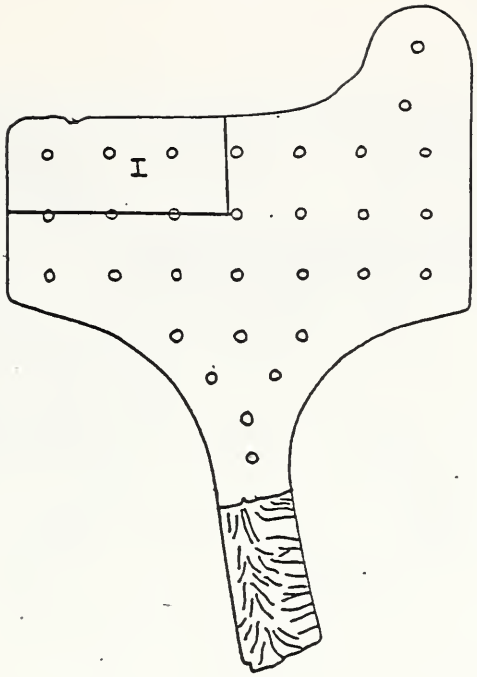

Figure 10. Schematic drawing of wheel piece F1SA2 showing the location of section I.

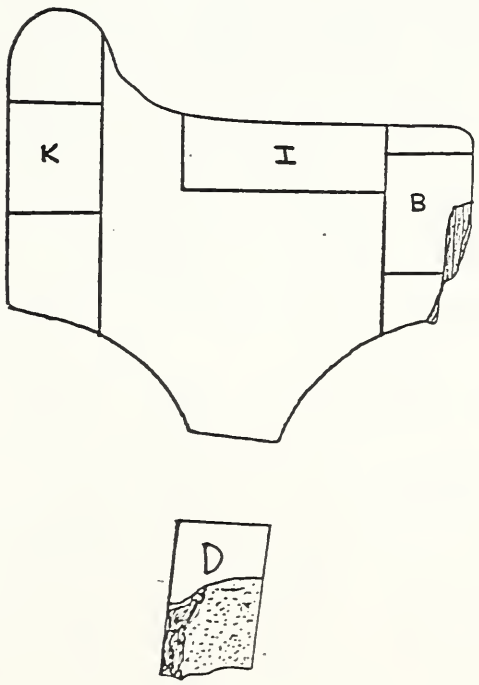

Figure 11. Schematic drawing of wheel piece F2SB2 showing the location of sections K, I, B, and D.

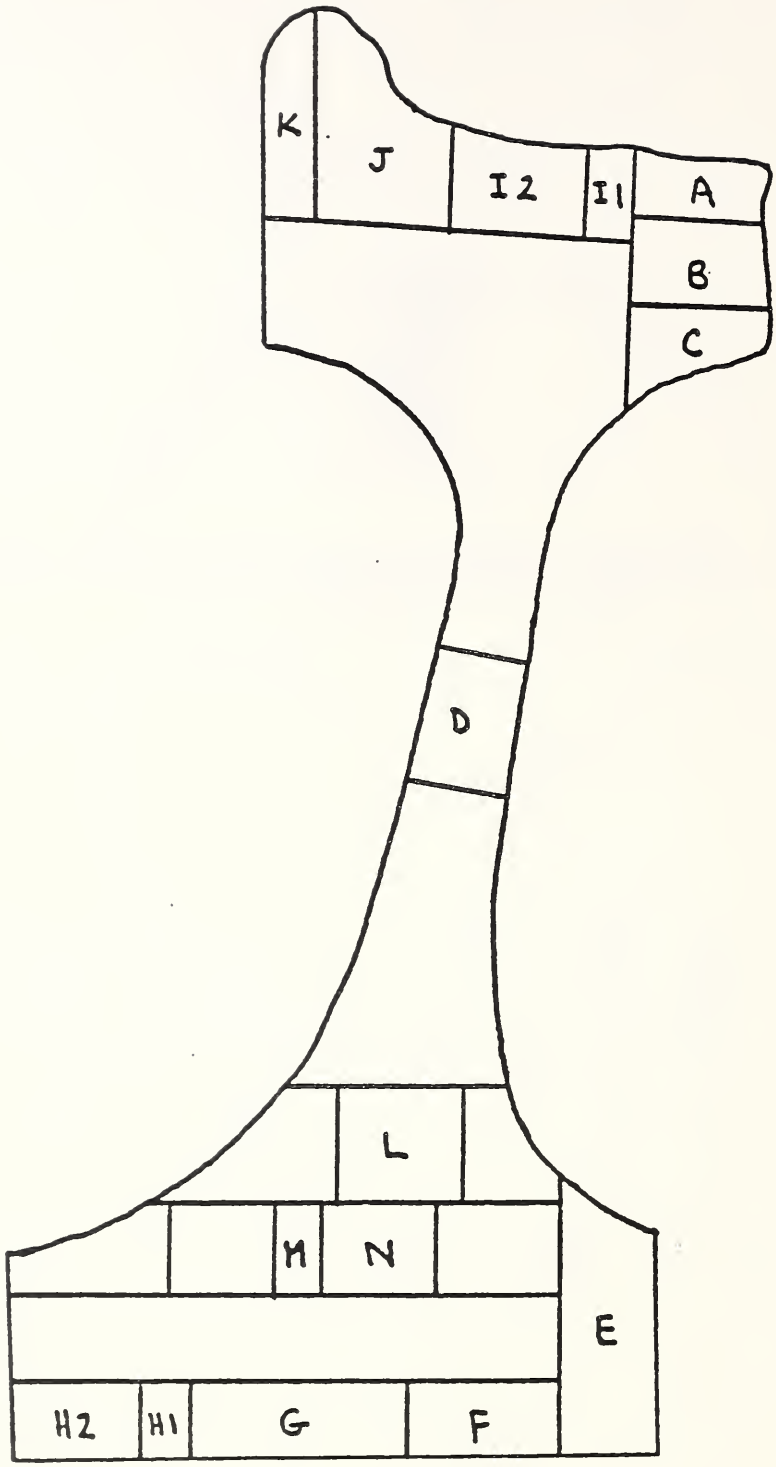

Figure 12. Schematic drawing showing the locations where the various sections were removed from wheel piece F2LA2.

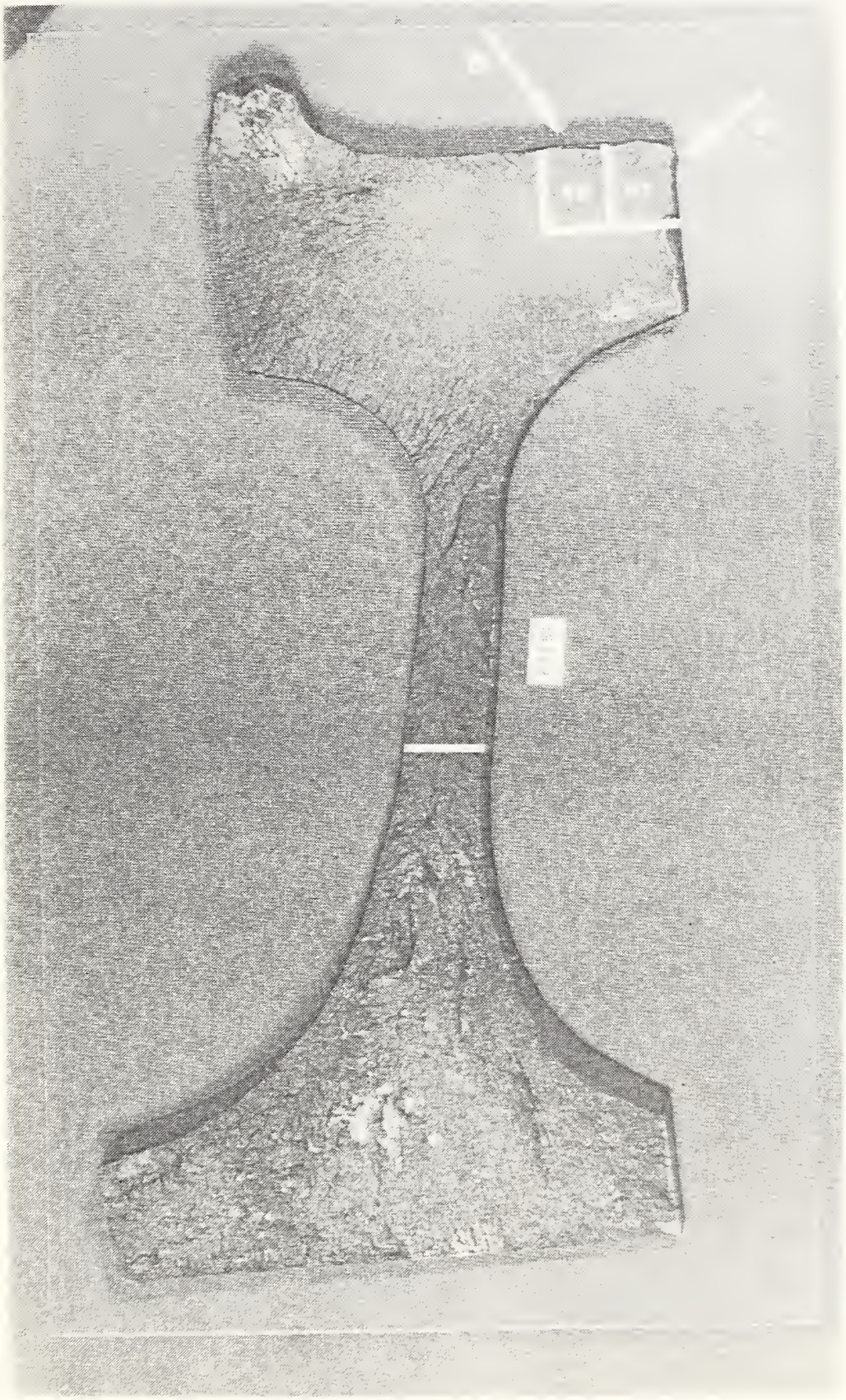

Figure 13. Fracture surface of wheel piece F2SB1 showing the location of sections A1 and A2, and the lower part which was returned to the FRA.

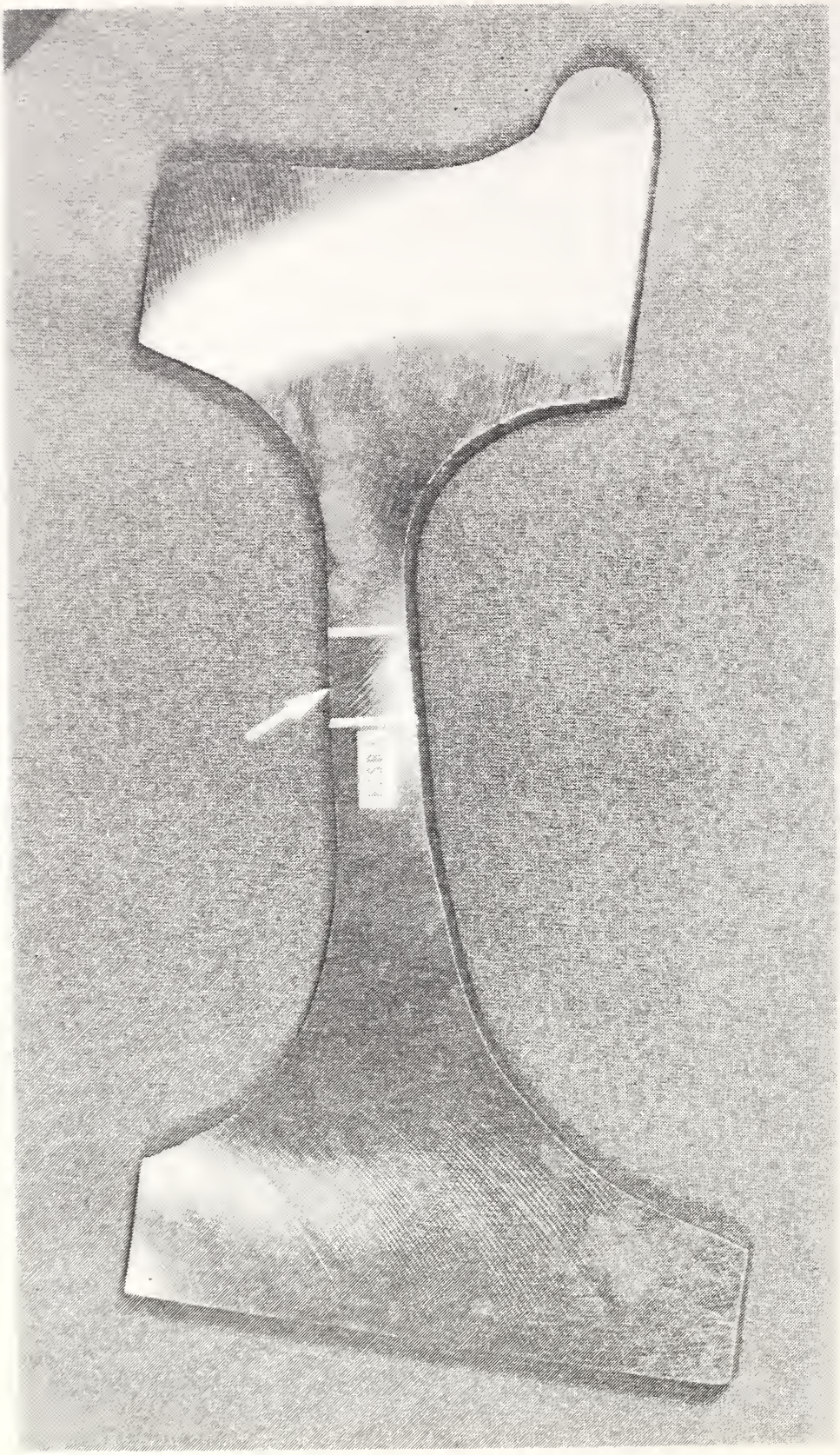

Figure 14. Wheel section F2SB2 showing the location of the sample taken for chemical analysis.

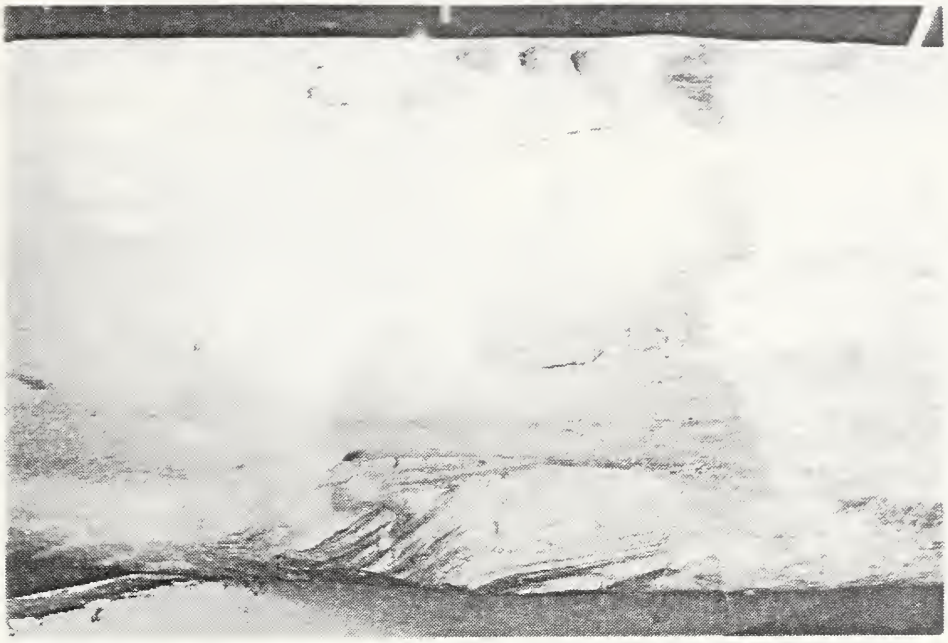

Figure 15. Severely abraded region of the tread of wheel piece F1L.

Figure 16. Severely galled region of the tread of wheel piece F1L.

Figure 17. Example of gouging of the tread of wheel piece F1L.

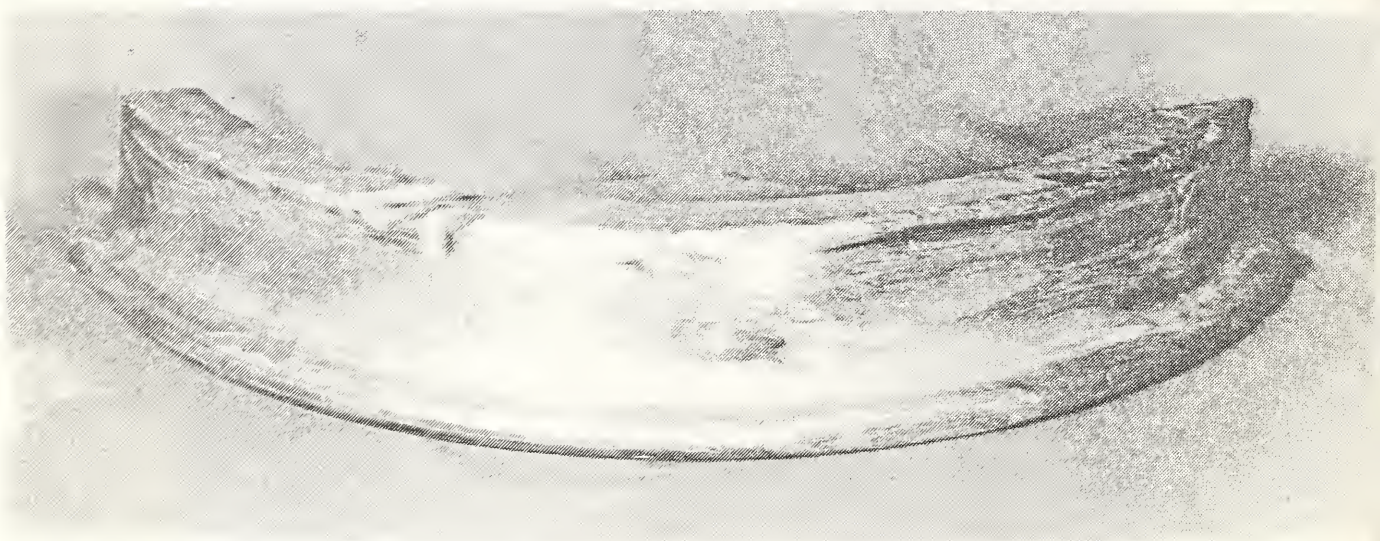

Figure 18. Wheel piece F1S with the outside of the wheel facing up showing mechanical damage to the tread and outside of the wheel adjacent to the tread.

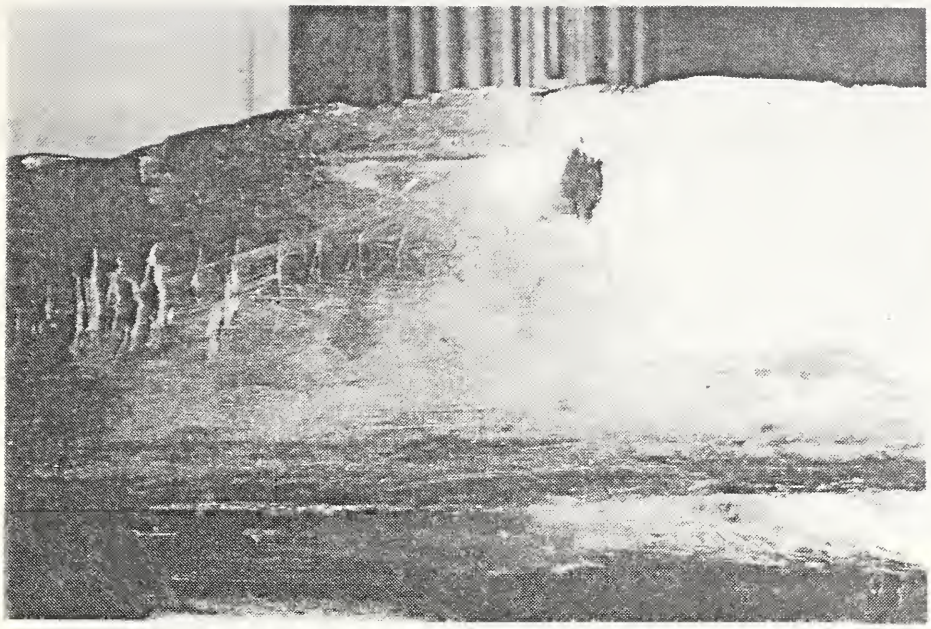

Figure 19. Region of the tread of wheel piece F1S exhibiting galling and gouging.

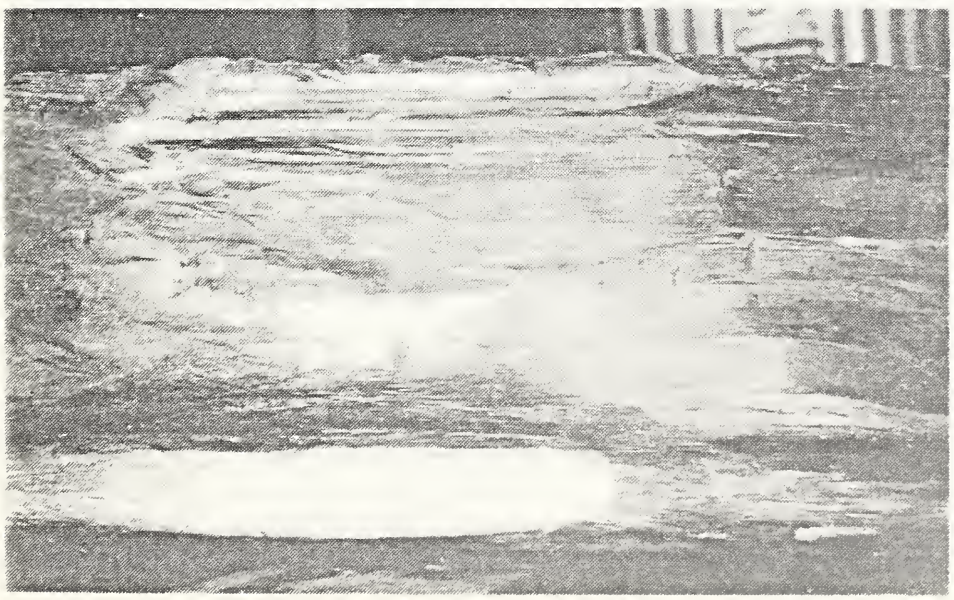

Figure 20. Flat spot on the tread of wheel piece F1S.

Figure 21. Example of mechanical damage on the tread of wheel piece F2L.

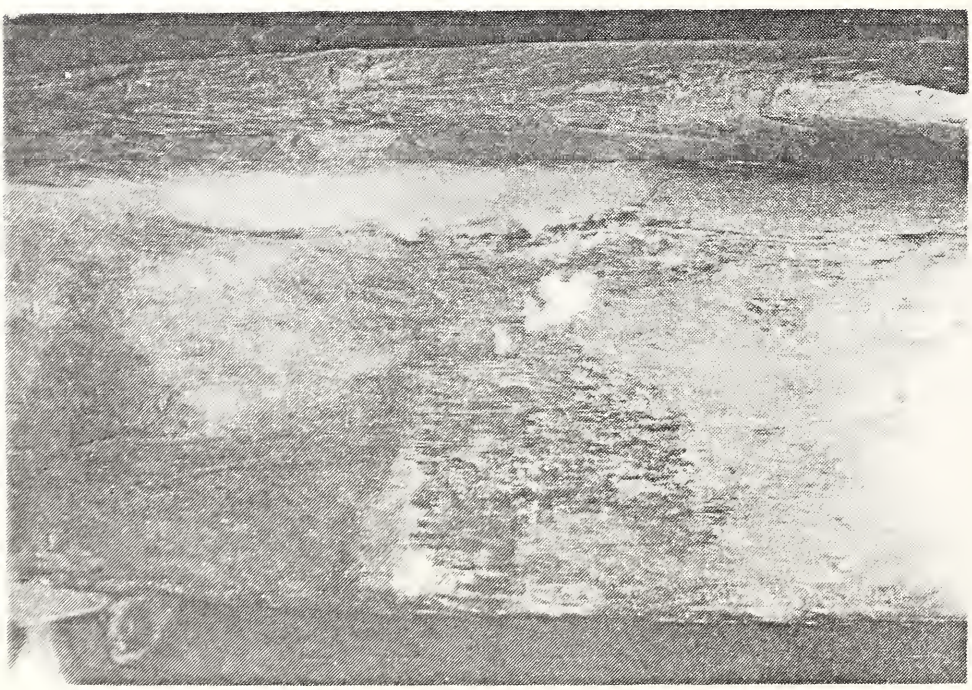

Figure 22. Mechanical damage on the tread of wheel piece F2S.

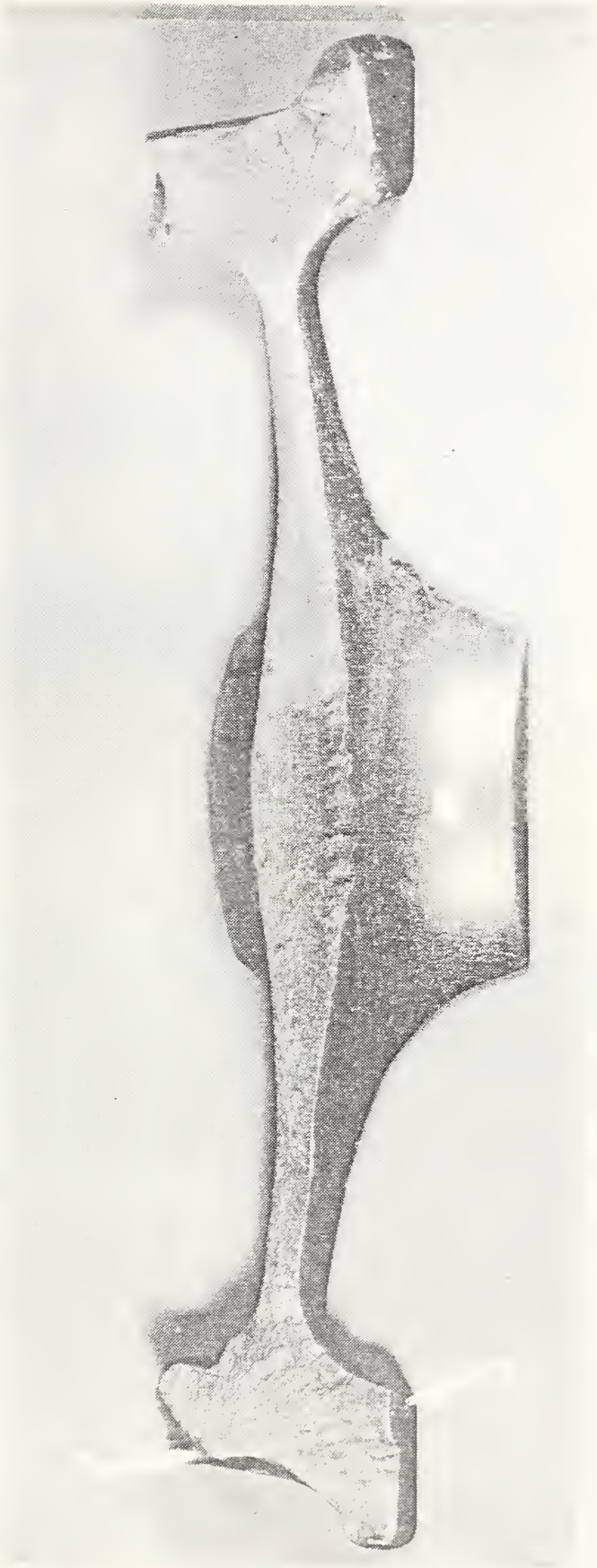

Figure 23. Fracture surface of wheel piece F1LB1. Arrow A indicates region of probable fracture initiation. Arrow B indicates depression common to both mating wheel pieces F1L and F1S.

Figure 24. Wheel piece F1SA1 showing part of the fracture corresponding to the mating fracture shown in figure 21. The arrow indicates the depression that was exhibited by both fractured pieces F1L and F1S. X1/2

Figure 25. Fracture surface of specimen A1 from wheel piece F2SB1 in the region of the fracture initiation. X6

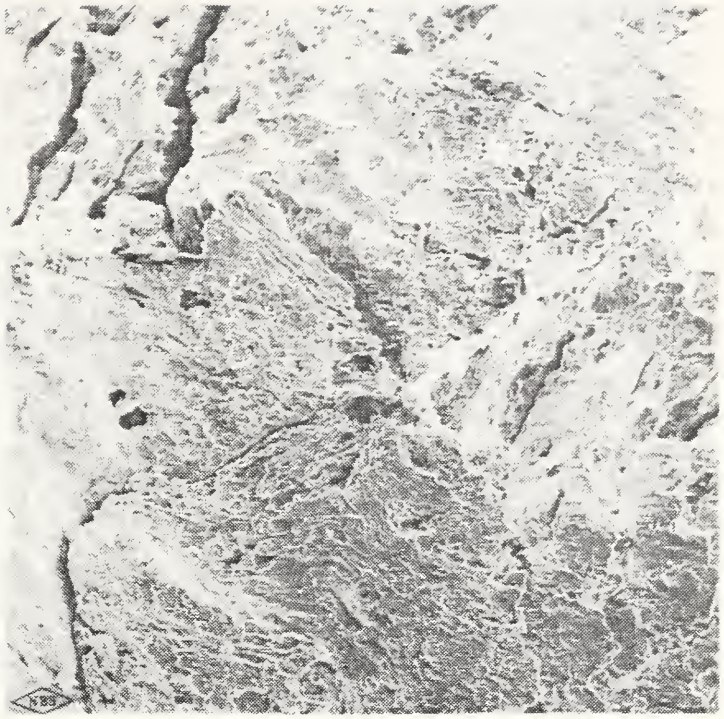

Figure 26. SEM fractograph of the "smeared" region of specimen A1 from wheel piece F2SB1. Grain boundary cracking is evident. X500

Figure 27. SEM fractograph of a region adjacent to the smeared region of specimen A1 from wheel piece F2SB1. Cleavage is the predominant fracture mode. X500

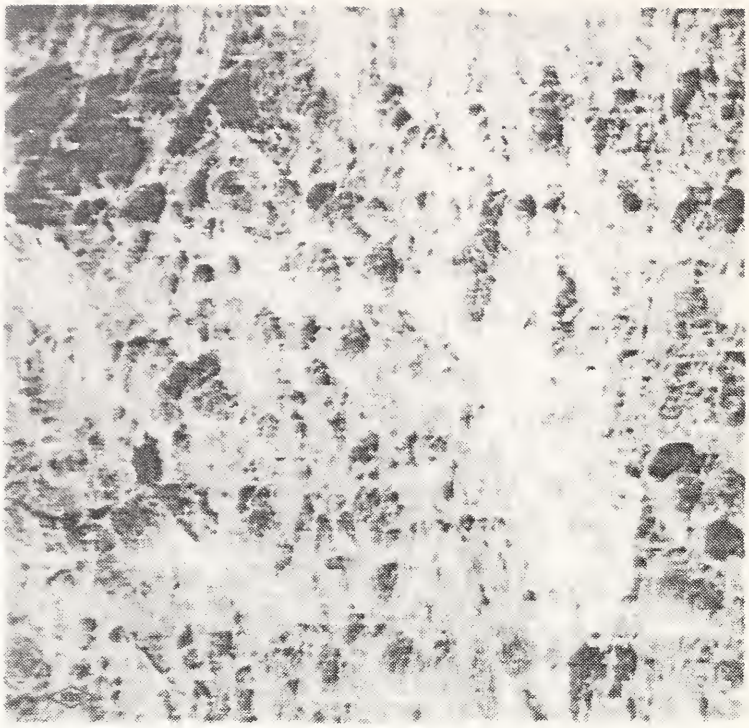

Figure 28. SEM fractograph representative of the heavily oxidized region of specimen A2 from wheel piece F2SB1. The effects of corrosion can be seen. X500

Figure 29. SEM fractograph from specimen A2 in a region near the tread, but removed from the heavily oxidized area. Cleavage is the predominant fracture mode. X500

Figure 30. SEM fractograph in a region well removed from the tread of specimen A2 from wheel piece F2SB1. X500

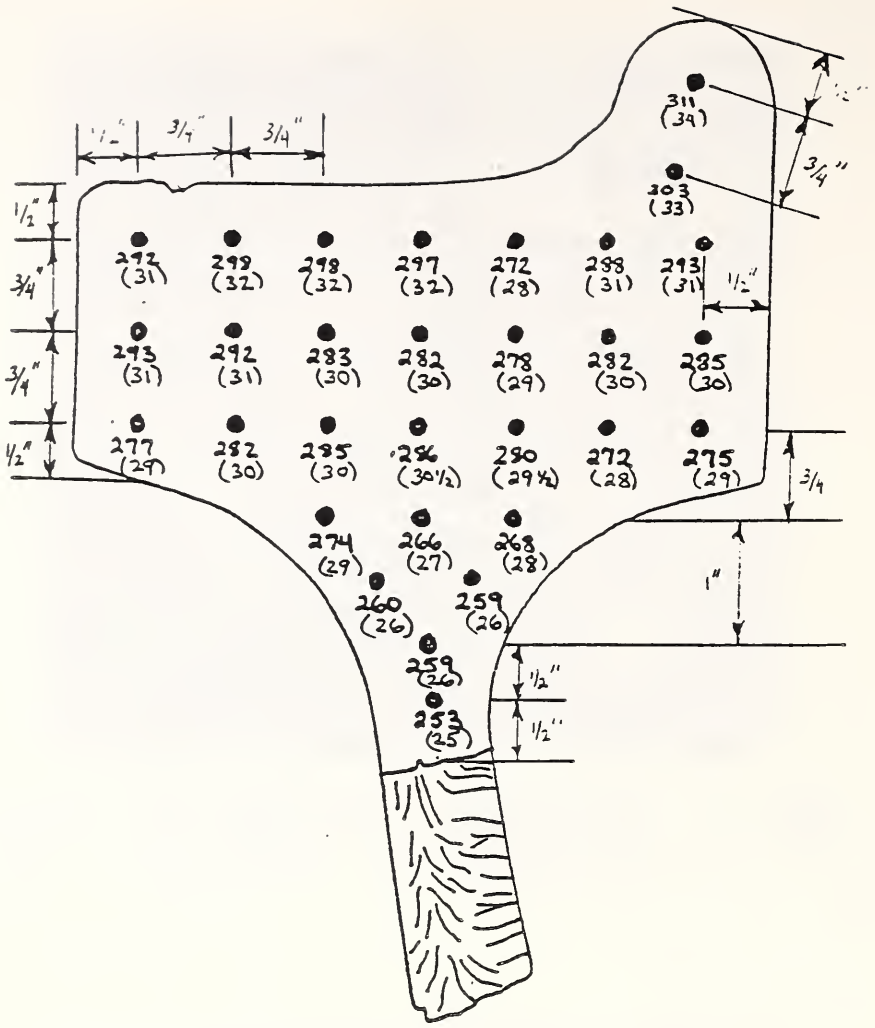

Figure 31. Brinell hardness measurement results on wheel piece F1SA2. The numbers in parentheses are approximate Rockwell C equivalent hardness values.

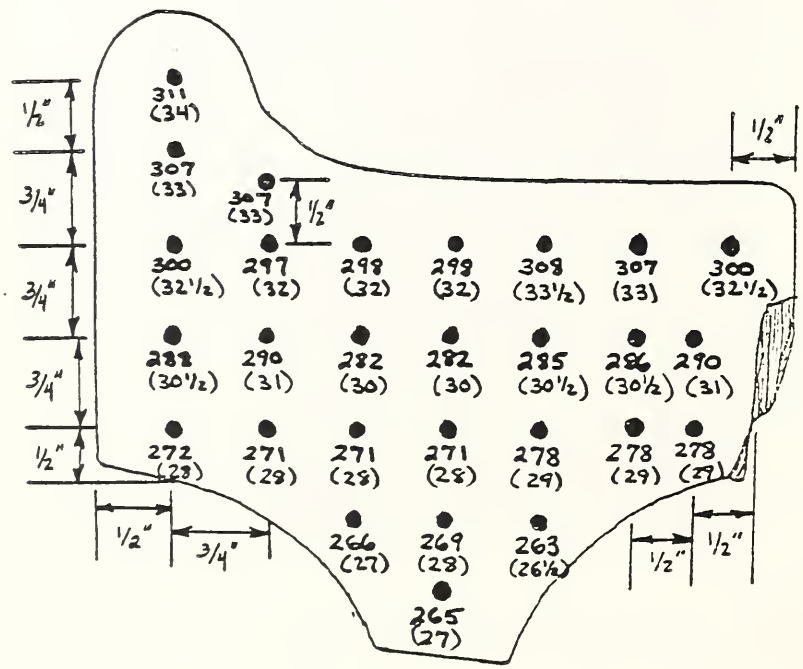

Figure 32. Brinell hardness measurement results on wheel piece F1SB2. The numbers in parentheses are approximate Rockwell C equivalent values.

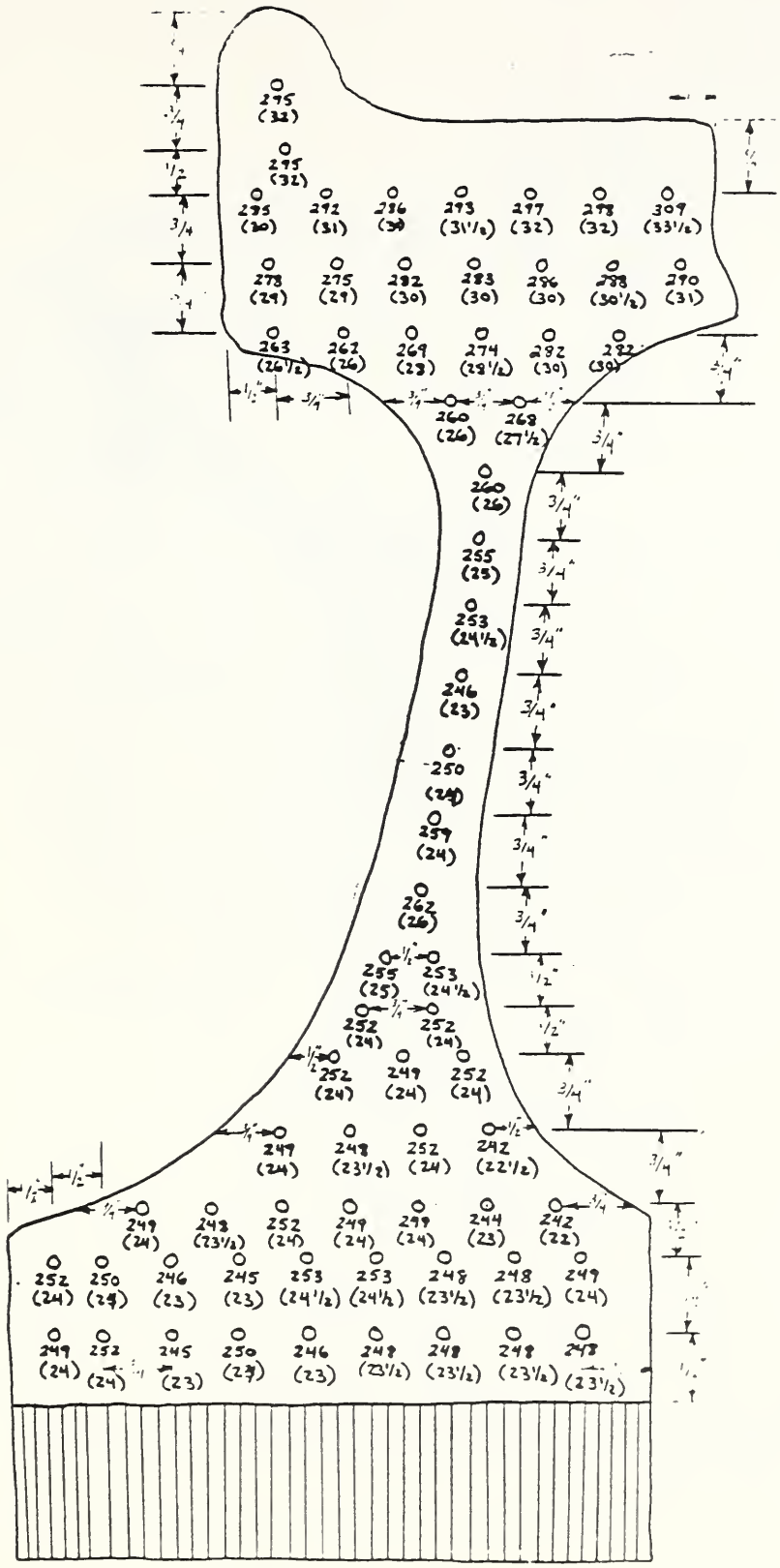

Figure 33. Brinell hardness measurement results on wheel piece F1LB2. Approximately equivalent Rockwell C hardness values are given in parentheses.

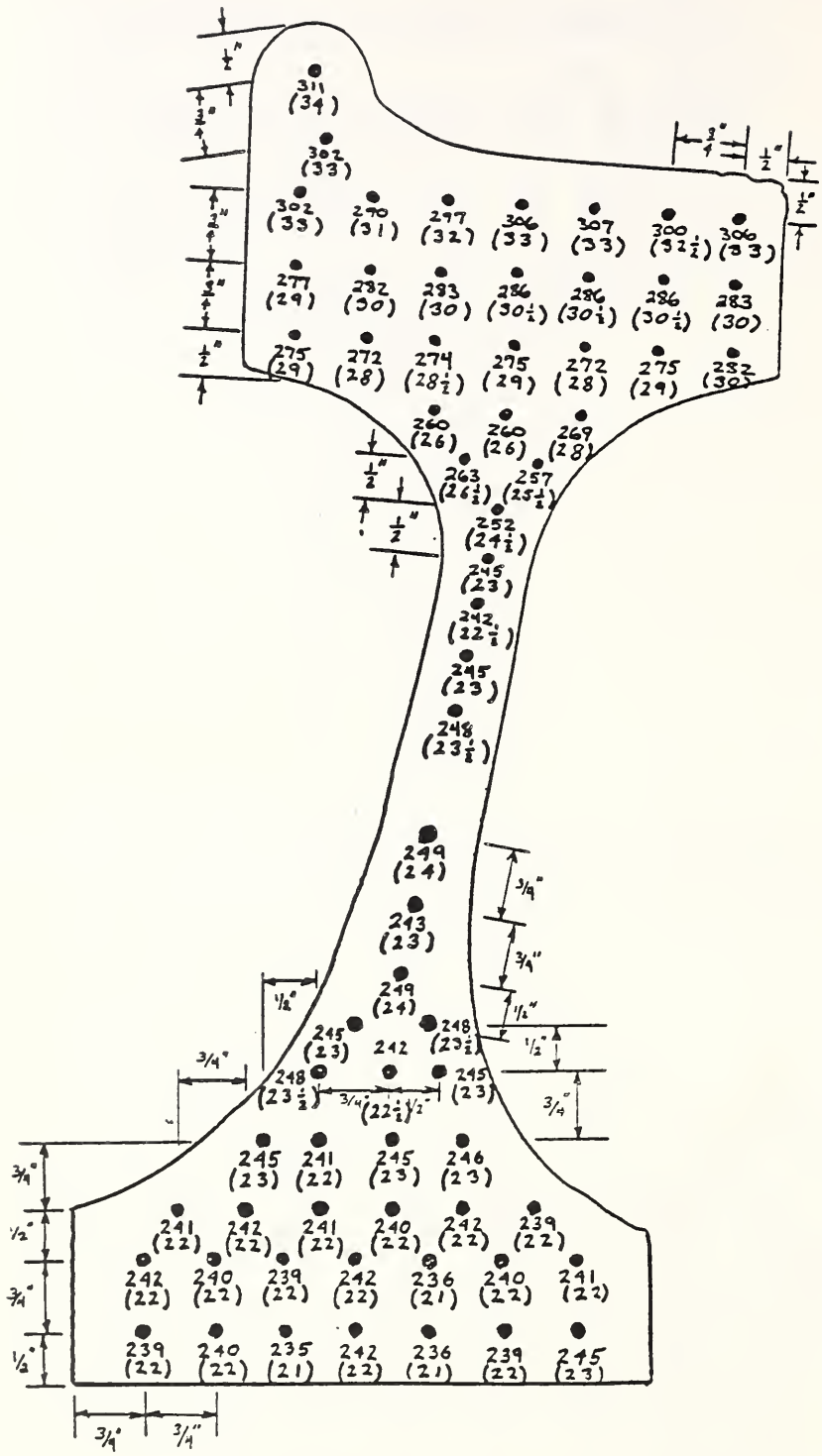

Figure 34. Brinell hardness measurement results on wheel piece F2SB2. Approximately equivalent Rockwell C hardness values are given in parentheses.

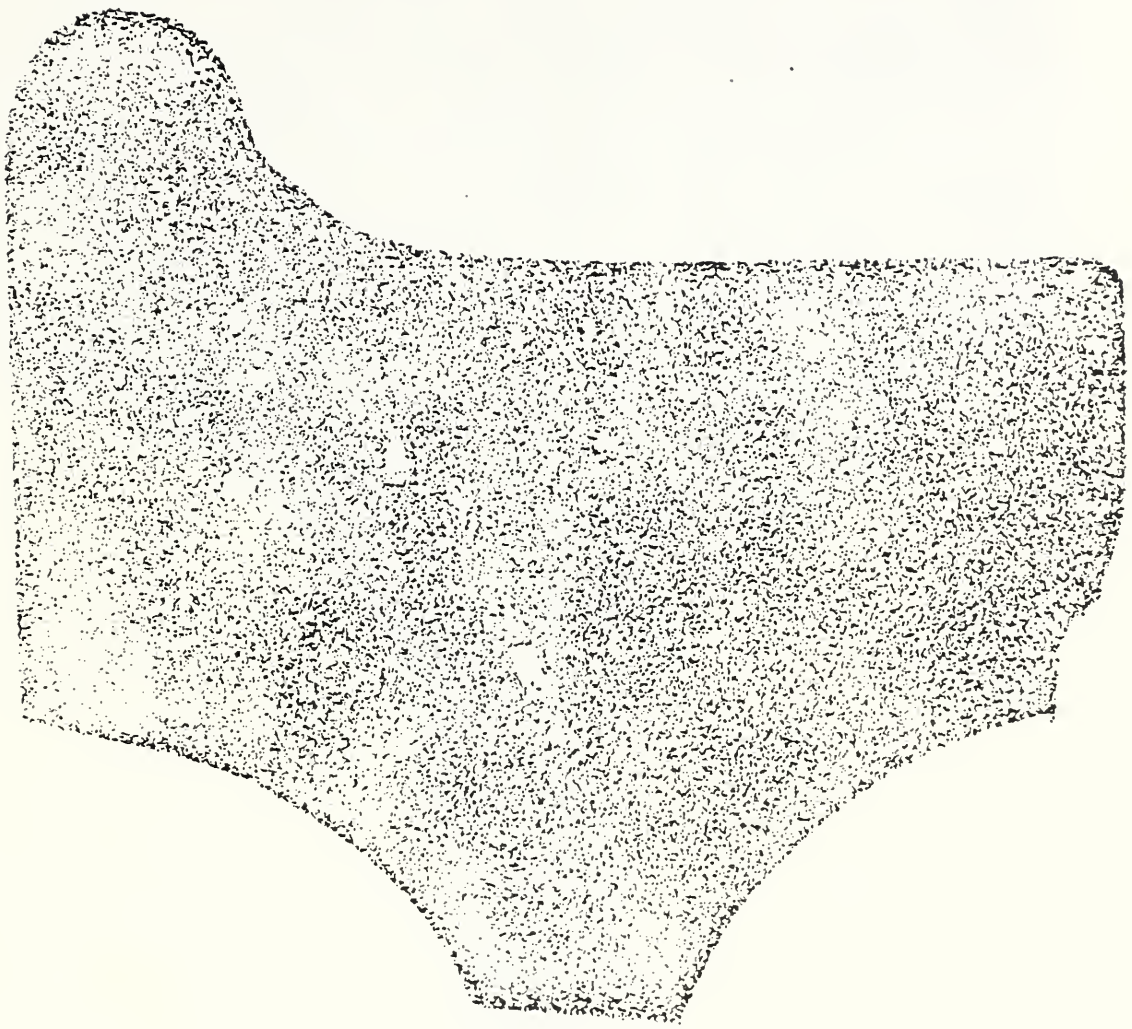

Figure 35. Sulfur print from wheel piece F1SB2.

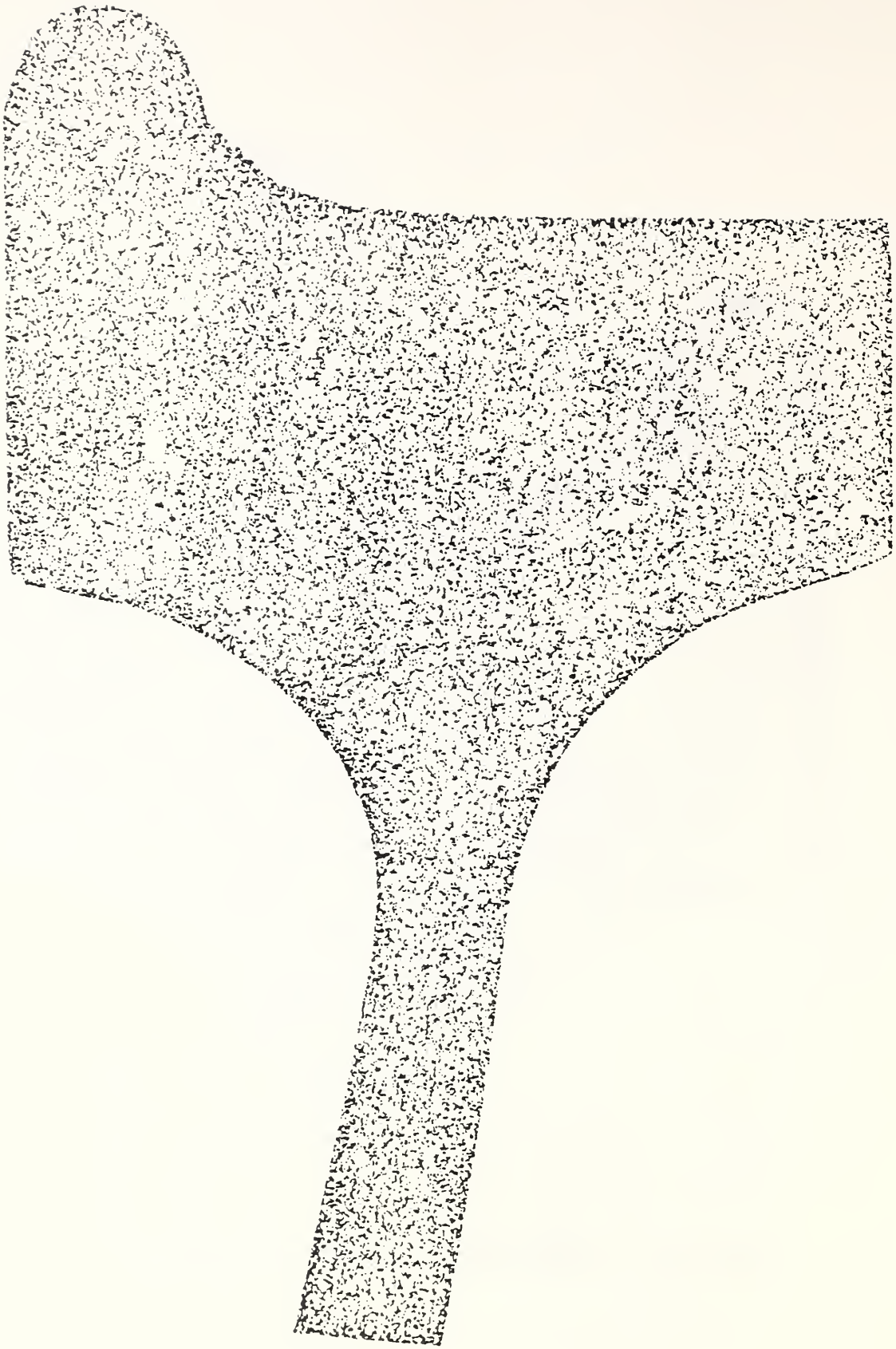

Figure 36. Sulfur print from wheel piece F1LB4.

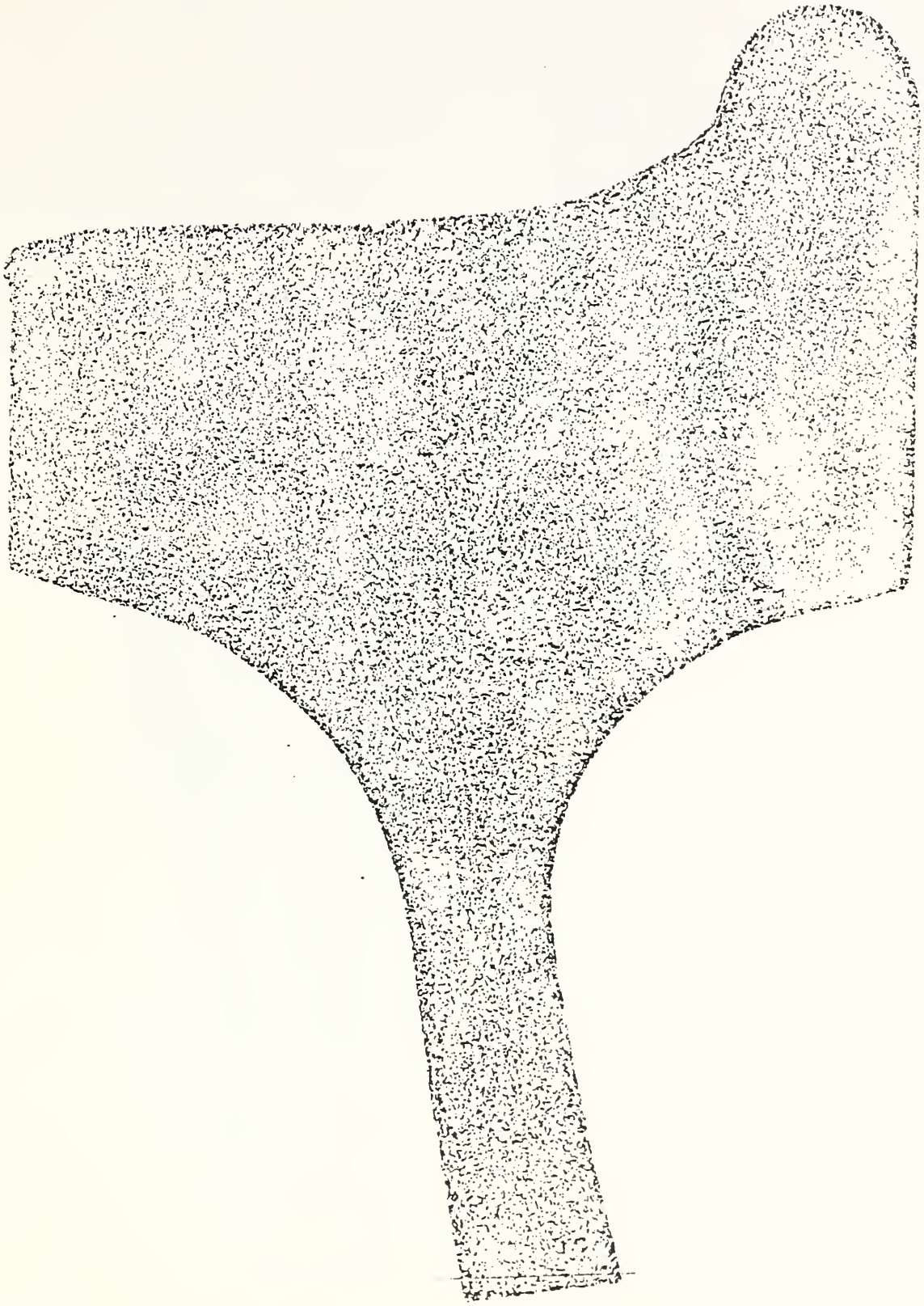

Figure 37. Sulfur print from wheel piece F2SB2.

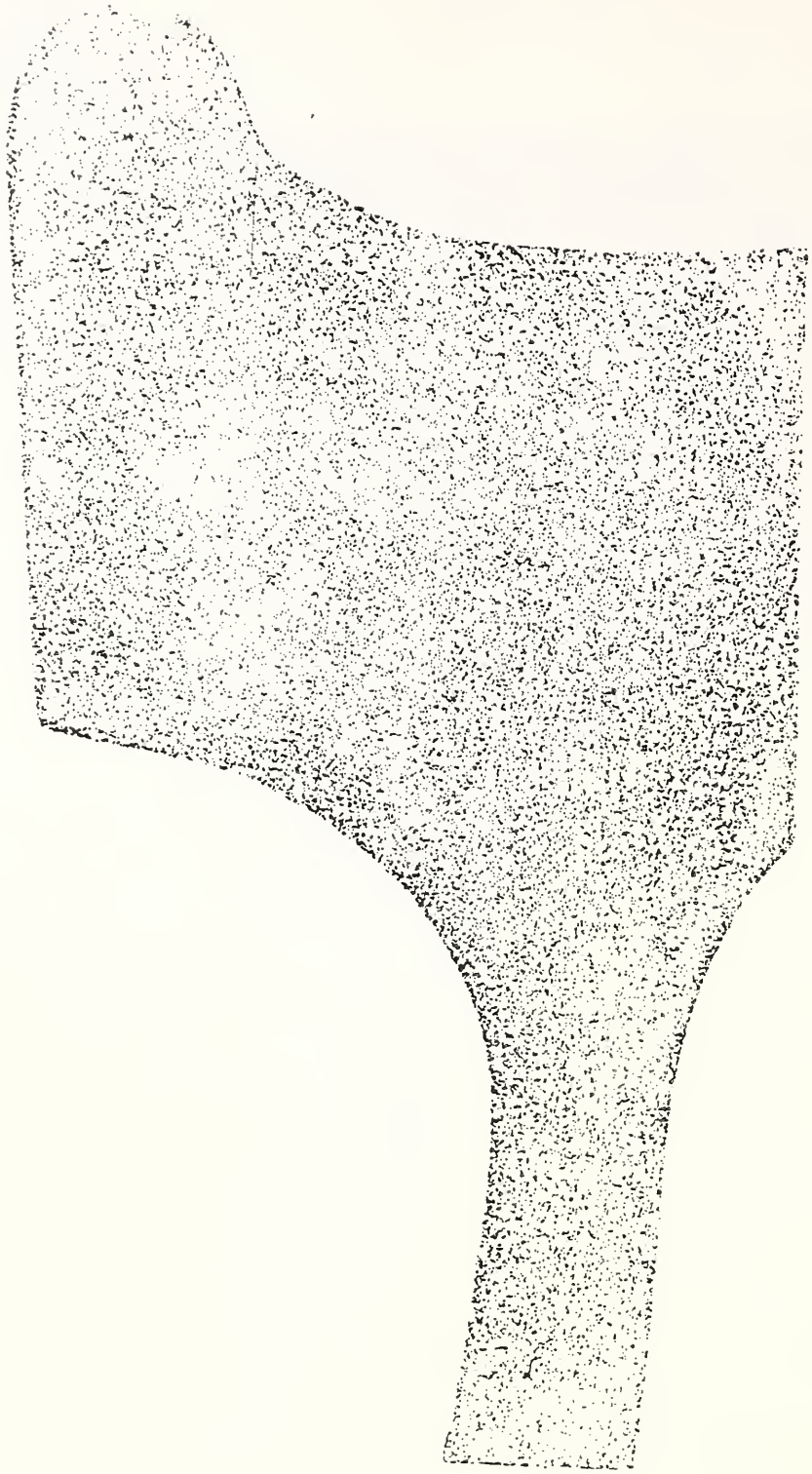

Figure 38. Sulfur print from wheel piece F2LA2.

Figure 39. Metallographically prepared area from wheel piece F1SB2-D used for inclusion rating. As-polished. X100

Figure 40. Metallographically prepared area from wheel piece F2LA2-A used for inclusion rating. As-polished. X100

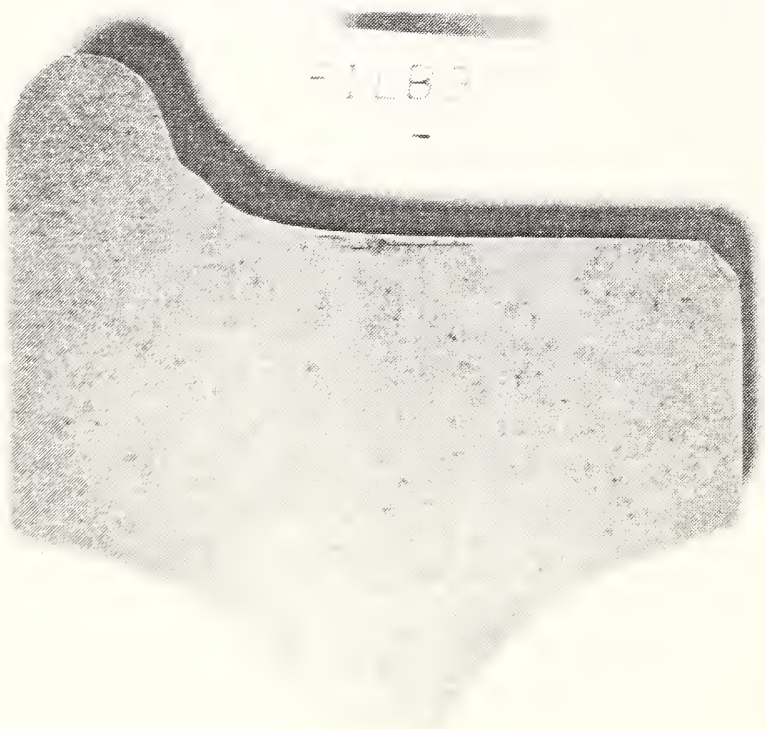

Figure 41. Wheel piece F1LB3 deep etched showing crack parallel and adjacent to the tread. Etchant: Boiling 50% HC1, 50% H_2O

Figure 42. Wheel piece F2LA2 etched to reveal the region of the tread that had been overheated. Etchant: 2% nital

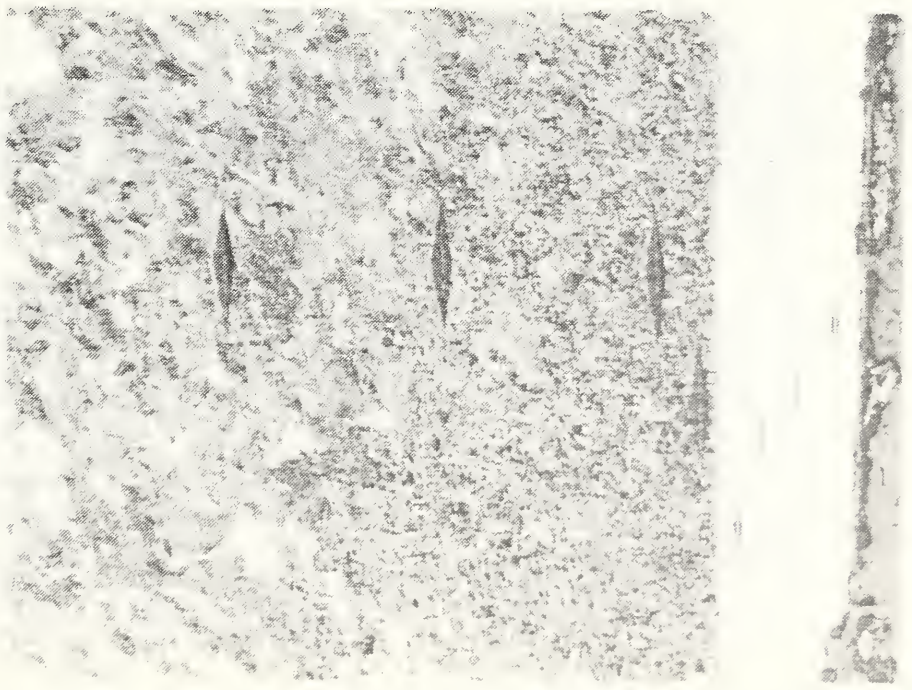

Figure 43. Wheel piece F2SB1 showing the overheated region at the tread (white in figure) in a different area of the wheel and at higher magnification than in figure 42. (The diamond shaped regions are Knoop microindentation hardness impressions.) Etchant: Sodium persulphate X200

Figure 44. Representative area from the overheated region of the tread of wheel piece F2LA2, specimen A exhibiting martensite.
Etchant: 2% nital X1000

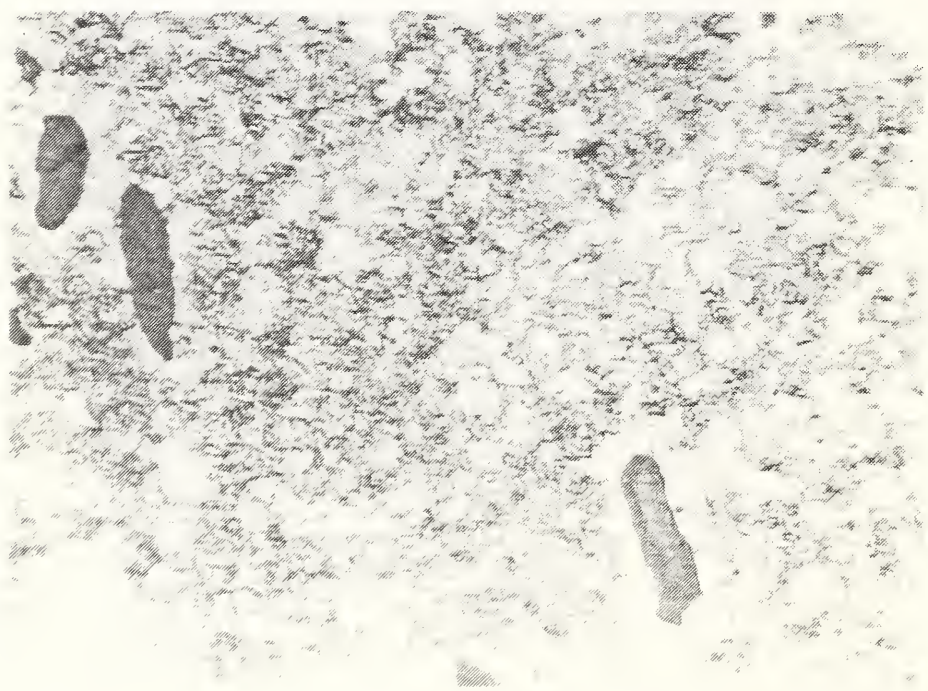

Figure 45. Representative area from the transition region between the heat affected zone and the unaffected base material.
Etchant: 2% nital X1250

Figure 46. Representative microstructure of wheel piece F2LA2 away from the tread.
Etchant: 2% nital X100

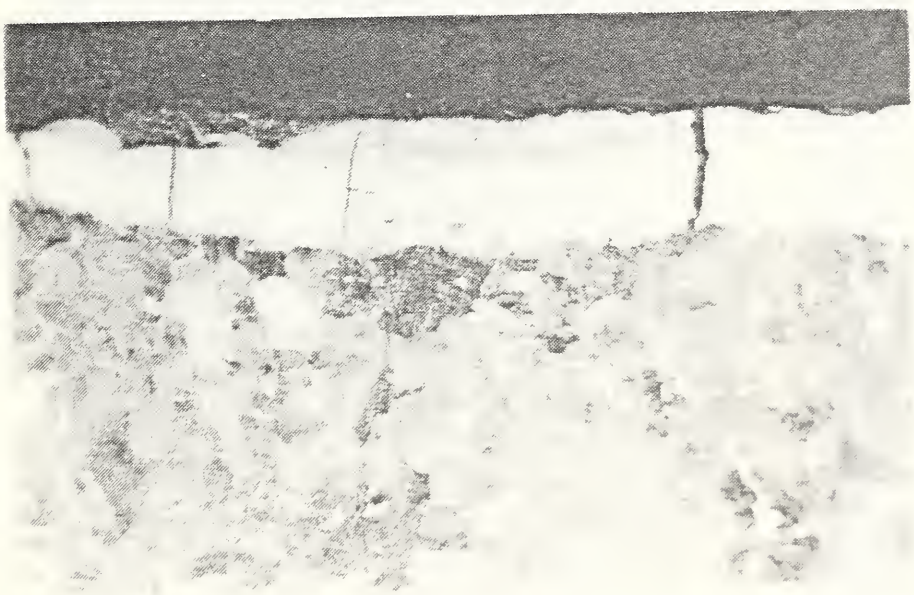

Figure 47. Microstructure of wheel piece F2LA2 at the hub showing an overheated area (white) with radial cracks.
Etchant: 2% nital X500

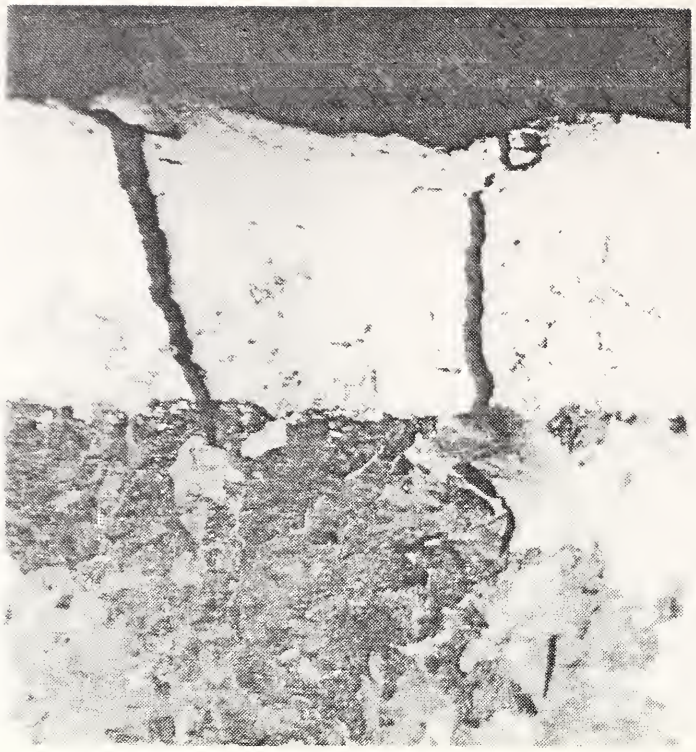

Figure 48. Heat affected area at the hub of wheel piece F2LA2 showing cracks penetrating into material unaffected by overheating.
Etchant: 2% nital X500

Figure 49. Cracks at inclusion near tread surface (horizontal at the top in the figure) of wheel piece F2SB1-A2.
Etchant: Picral X1000

Figure 50. Crack at the tread surface of wheel piece F2SB1-A2 in a region close to the crack shown in Figure 49.
Etchant: Picral X1000

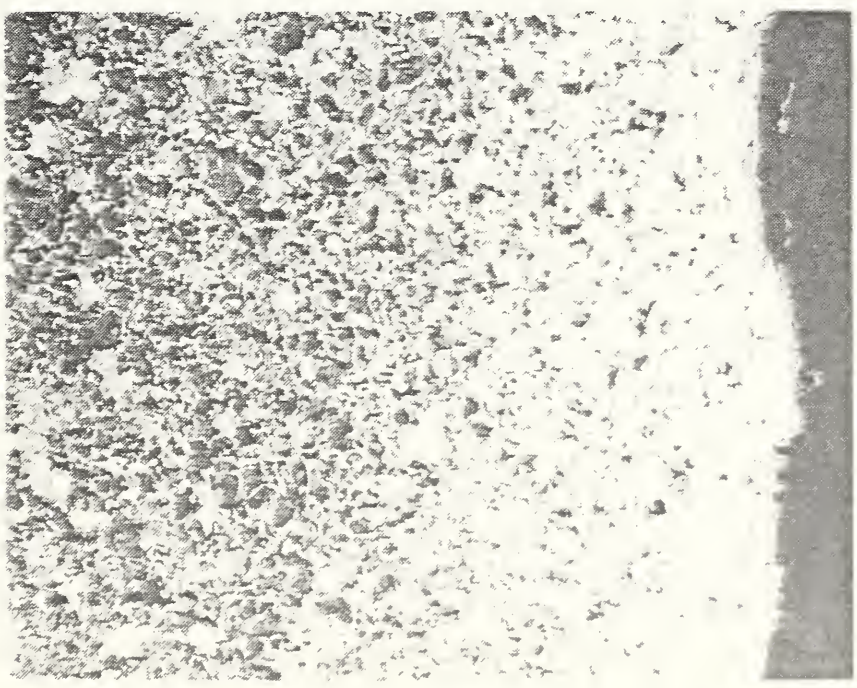

Figure 51. Inboard edge of the web of wheel piece F2LA2 showing decarburization near the surface.
Etchant: 2% nital X100

NBS-114A (REV. 2-8C)

U.S. DEPT. OF COMM. BIBLIOGRAPHIC DATA SHEET (See instructions)	1. PUBLICATION OR REPORT NO. NBSIR 86-3383	2. Performing Organ. Report No.	3. Publication Date

4. TITLE AND SUBTITLE

Examination of Failed Railroad Car Wheel/Axle Assembly from Derailed Passenger Car McIntosh, Georgia

5. AUTHOR(S)

T.R. Shives, S.R. Low, III, and C.H. Brady

6. PERFORMING ORGANIZATION (If joint or other than NBS, see instructions)

NATIONAL BUREAU OF STANDARDS
DEPARTMENT OF COMMERCE
WASHINGTON, D.C. 20234

7. Contract/Grant No.

8. Type of Report & Period Covered

9. SPONSORING ORGANIZATION NAME AND COMPLETE ADDRESS (Street, City, State, ZIP)

10. SUPPLEMENTARY NOTES

☐ Document describes a computer program; SF-185, FIPS Software Summary, is attached.

11. ABSTRACT (A 200-word or less factual summary of most significant information. If document includes a significant bibliography or literature survey, mention it here)

At the request of the Federal Railroad Administration, the National Bureau of Standards conducted an examination of a failed wheel assembly from an Amtrak passenger car involved in a derailment at McIntosh, Georgia. The west lead wheel of the trailing truck of the car was found to have a radial fracture which permitted the wheel to move laterally along the axle. The east wheel had suffered a chordal fracture. The apparent sequence of events is the radial fracture of the west wheel followed by lateral motion of that wheel along the axle which permitted the east wheel to drop in the gauge of the track causing the derailment. The fracture of the east wheel was thought to be a result of the derailment.

The west wheel fractured from a crack that initiated at the outside of the tread. There was evidence of a pre-existing crack in the fracture path near the fracture origin, although it is not clear that this crack initiated the fracture. The fracture of the east wheel also initiated at the outside of the tread. There was a gouge near the fracture origin and the fracture passed through a dent, but it is not clear that there is any relationship between either of these areas of mechanical damage and the fracture.

In addition to the fracture crack, two radial cracks were found at the tread of the west wheel. One of these cracks was associated with an inclusion. Although both wheels appear basically to satisfy AAR specification for B-36 wheels, some dimensions did not comply and hardness of the west wheel was marginal in a couple of instances.

12. KEY WORDS (Six to twelve entries; alphabetical order; capitalize only proper names; and separate key words by semicolons)

Derailment; fracture; fracture initiation; railroad accident; railroad wheel; railroad wheel fracture

13. AVAILABILITY

☐ Unlimited

☒ For Official Distribution. Do Not Release to NTIS

☐ Order From Superintendent of Documents, U.S. Government Printing Office, Washington, D.C. 20402.

☐ Order From National Technical Information Service (NTIS), Springfield, VA. 22161

14. NO. OF PRINTED PAGES

55

15. Price

$11.95

USCOMM-DC 6043-P80